Article

Cell

Intrinsically Disordered Proteins Drive Emergence and Inheritance of Biological Traits

Graphical Abstract

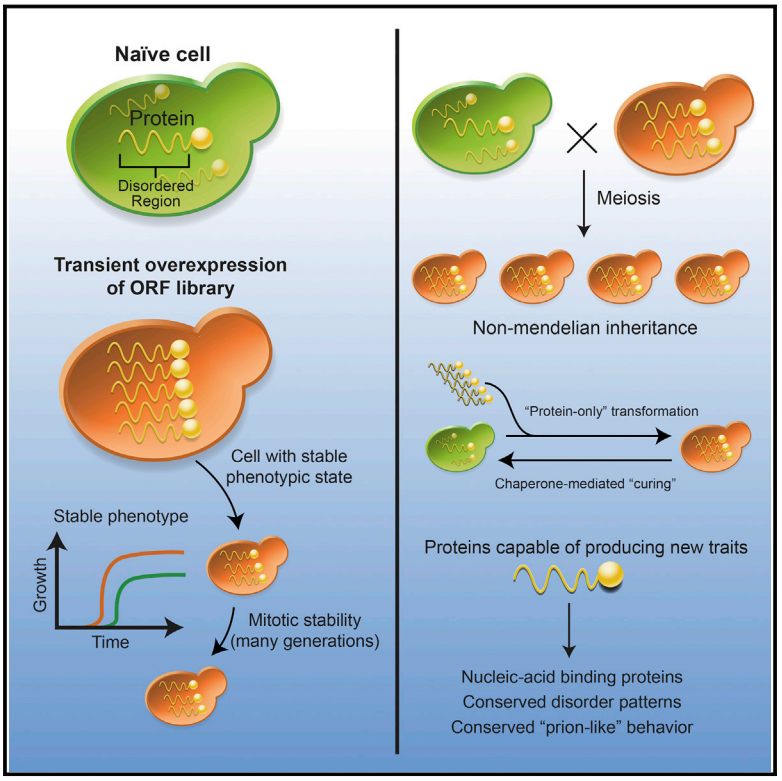

Highlights

- Transient overexpression of many yeast proteins creates heritable biological traits
- The traits have prion-like inheritance patterns and can involve gains of function
- The traits are transmissible by protein only but do not arise from amyloid fibers
- The traits arise from disordered protein sequences conserved from yeast to man

Authors

Sohini Chakrabortee, James S. Byers, Sandra Jones, ..., Brayon Fremin, Susan Lindquist, Daniel F. Jarosz

Correspondence

lindquist_admin@wi.mit.edu (S.L.), jarosz@stanford.edu (D.F.J.)

In Brief

Intrinsically disordered proteins act in a prion-like manner to create protein-based molecular memories that drive the emergence of new, frequently adaptive traits.

Chakrabortee et al., 2016, Cell *167*, 369–381
October 6, 2016
http://dx.doi.org/10.1016/j.cell.2016.09.017

CellPress

Cell

Intrinsically Disordered Proteins Drive Emergence and Inheritance of Biological Traits

Sohini Chakrabortee,[1,6,8] James S. Byers,[2,6] Sandra Jones,[1,9] David M. Garcia,[3] Bhupinder Bhullar,[1,10] Amelia Chang,[4,11] Richard She,[3] Laura Lee,[4] Brayon Fremin,[3,7] Susan Lindquist,[1,5,*] and Daniel F. Jarosz[2,3,12,*]
[1]Whitehead Institute for Biomedical Research, Cambridge, MA 02142, USA
[2]Department of Developmental Biology
[3]Department of Chemical and Systems Biology
[4]Department of Biology
Stanford University, Stanford, CA 94305, USA
[5]HHMI and Department of Biology, MIT, Cambridge, MA 02139, USA
[6]Co-first author
[7]Present address: Department of Genetics, Stanford University, Stanford, CA 94305, USA
[8]Present address: University of Birmingham, Edgbaston, Birmingham B15 2SQ, UK
[9]Present address: The Rockefeller University, New York, NY 10065, USA
[10]Present address: Novartis Institute for Biomedical Research, 4002 Basel, Switzerland
[11]Present address: Harvard Medical School, Boston, MA 02118, USA
[12]Lead Contact
*Correspondence: lindquist_admin@wi.mit.edu (S.L.), jarosz@stanford.edu (D.F.J.)
http://dx.doi.org/10.1016/j.cell.2016.09.017

SUMMARY

Prions are a paradigm-shifting mechanism of inheritance in which phenotypes are encoded by self-templating protein conformations rather than nucleic acids. Here, we examine the breadth of protein-based inheritance across the yeast proteome by assessing the ability of nearly every open reading frame (ORF; ~5,300 ORFs) to induce heritable traits. Transient overexpression of nearly 50 proteins created traits that remained heritable long after their expression returned to normal. These traits were beneficial, had prion-like patterns of inheritance, were common in wild yeasts, and could be transmitted to naive cells with protein alone. Most inducing proteins were not known prions and did not form amyloid. Instead, they are highly enriched in nucleic acid binding proteins with large intrinsically disordered domains that have been widely conserved across evolution. Thus, our data establish a common type of protein-based inheritance through which intrinsically disordered proteins can drive the emergence of new traits and adaptive opportunities.

INTRODUCTION

Our understanding of protein-based inheritance is still in its infancy, and insights have been gleaned from just a handful of examples. Biochemical and genetic studies have established that prion proteins have the ability to adopt multiple stable conformations, at least one of which self-perpetuates. This unusual folding landscape allows prions to create heritable changes in phenotype as protein-based genetic elements. However, the evolutionary breadth of this mechanism is unknown, and its biological significance is highly controversial (McGlinchey et al., 2011; Nakayashiki et al., 2005). Although some prions have been proposed to have adaptive value (Jarosz et al., 2014a; Khan et al., 2015; Suzuki et al., 2012; True and Lindquist, 2000), this paradigm-shifting mechanism of inheritance was discovered as a mechanism for the transmission of a devastating spongiform encephalopathy (Prusiner, 1982).

At the molecular level, virtually all known prions produce new traits by forming highly stable cross-beta-sheet amyloid fibers (Balbirnie et al., 2001; Glover et al., 1997; King et al., 1997). Propagation of these traits, and the amyloids that confer them, relies on the severing of prion templates into smaller "seeds" by the protein-remodeling factor Hsp104 (Chernoff et al., 1995). These seeds are passed from mother cells to their daughters, serving as "replicons" to template future rounds of assembly (Chernoff et al., 1995; Shorter and Lindquist, 2004). Thus, transiently inhibiting Hsp104 heritably eliminates the prion state (Ferreira et al., 2001). Because their inheritance involves self-templating changes in protein conformation, [*PRION*$^+$]-based traits have very different patterns of inheritance in genetic crosses than chromatin-based traits: their phenotypes are dominant (denoted by capital letters) and segregate to meiotic progeny in a non-Mendelian fashion (denoted by brackets). Recent work has identified another type of cellular memory based on protein super-assemblies formed by the G1/S inhibitor Whi3 (Caudron and Barral, 2013). These "mnemons," in contrast to prions, are retained in mother cells at cytokinesis.

Systematic screens have identified additional prions and candidates (Alberti et al., 2009; Derkatch et al., 2001). These searches have generally relied on identifying proteins that share the features of known yeast prions such as [*PSI*$^+$] (Chernoff et al., 1995; Patino et al., 1996), [*URE3*] (Wickner, 1994), and [*RNQ*$^+$] (Derkatch et al., 2001; Sondheimer and Lindquist, 2000): (1) regions strongly enriched in asparagine (N) and glutamine (Q)

residues, (2) formation of amyloid fibers in their [*PRION*$^{+}$] form, and (3) an absolute requirement for Hsp104's amyloid-severing function for propagation. As revealing as these studies have been, they would not have identified the bona fide prions PrP (Prusiner, 1982), [Het-s] (Coustou et al., 1997), Mod5 (Suzuki et al., 2012), and [*GAR*$^{+}$] (Brown and Lindquist, 2009). Moreover, they were not designed to identify any other types of protein-based inheritance, even if they have prion-like properties (e.g., MAVS; Hou et al., 2011). Thus, protein-based inheritance might well be more widespread than presently appreciated.

As a consequence of the law of mass action, self-templating conformations can be permanently induced by transient overexpression of the proteins that encode them (Derkatch et al., 1996; Ter-Avanesyan et al., 1994; Wickner et al., 2006). Here, we screened the yeast proteome for the ability to elicit stable biological traits by transiently and individually inducing the expression of virtually every yeast open reading frame (ORF). As others have reported (Sopko et al., 2006), protein overexpression broadly altered yeast growth. However, for nearly 50 proteins, we found that heritable epigenetic states—"molecular memories" of past overexpression—persisted for hundreds of generations after expression levels returned to normal. These phenotypes were passed from mother cells to their daughters with prion-like patterns of inheritance. The vast majority had strong adaptive value in diverse environments. Many proteins with this capacity were transcription factors (TFs) and RNA-binding proteins (RBPs) and most were neither known prions nor N/Q rich. They did not form amyloid fibers, and their transmission did not depend on Hsp104. Instead, inducing proteins harbored intrinsically disordered regions that have been widely conserved across evolution. Homologous human proteins also had the capacity to form self-perpetuating assemblies. Therefore, our findings greatly expand the scope of protein-based inheritance in the transmission of biological information and suggest that this mode of inheritance might be broadly used to regulate gene expression.

RESULTS

Transient Overexpression of 80 Proteins Creates Stable and Heritable Traits

First, we individually and systematically overexpressed nearly every known ORF (~5,300 ORFs) in *S. cerevisiae* from a single-copy plasmid with a galactose-inducible promoter (Hu et al., 2007). We examined how this affected growth in ten different stress conditions, and using stringent cutoffs, we identified hundreds of proteins that altered growth reproducibly (Table S1; Figure S1). To eliminate false-positives, we re-transformed plasmids containing each hit into naive cells in quadruplicate and re-tested their overexpression traits: >95% repeated in all four replicates. After approximately ten generations, we stopped overexpression by plating cells to glucose media for an additional approximately ten generations of growth. In 80 cases, we observed traits in progeny whose ancestors had experienced transient protein overexpression that we did not observe in naive controls (Table S2). The specificity and reproducibility of these traits established that they were linked to specific biological effects of the proteins being overexpressed rather than to de novo mutations or induced genome instability.

Next, we eliminated the overexpression plasmid entirely (see Supplemental Information). For each of the 80 proteins, we picked eight individual colonies from the four replicate experiments (32 total), grew them to saturation in non-selective media (SD-CSM), and compared their phenotypes to colonies whose ancestors had not experienced protein overexpression. Through these experiments, we identified 46 proteins that created stable epigenetic states that persisted for ~100 generations after overexpression was stopped (including ~50 generations without the plasmid). Proteins that elicited these traits were not merely long lived; they had significantly shorter half-lives than average for the yeast proteome ($p = 0.0006$ by t test; Belle et al., 2006). However, even if all of the induced proteins had been retained for 100 generations, it would have been diluted by 1-trillion-fold at the end of the experiment. The traits were robust to freeze-thaw, successive streaks on plates, and long-term liquid culture. Therefore, we conclude that they arose from stable "molecular memories" induced by past, transient changes in protein abundance. Notably, the proteins capable of effecting these traits were enriched in factors that regulate information flow, in particular, TFs and RBPs ($p = 0.0002$ by Fisher's exact test; annotations are from the Saccharomyces Genome Database).

Eleven of the Heritable Phenotypic States Are Regulated by Hsp104

Most known protein-based elements of inheritance are prions. Prion-based traits are distinguished from those that arise from mutations or other forms of epigenetic inheritance by their extreme reliance on agents that modulate protein conformations—notably, Hsp104 (Chernoff et al., 1995; Shorter and Lindquist, 2004). Therefore, we examined whether transient Hsp104 inhibition could eliminate the traits that emerged in our screen. We picked multiple colonies expressing each trait and passaged them three times on a rich medium (YPD) containing low doses of the Hsp104 inhibitor guanidine hydrochloride (GdnHCl). We then passaged them for 25 generations in standard medium to restore Hsp104 function. A quarter of these 46 traits (11) were dependent on Hsp104 (Figures 1A and 1B; Figure S1C; Table S3; see Table S4 for genetic confirmation). Most were neither known prions nor Q/N rich; and only two, Rbs1 and Scd5, harbored prion-like domains (Alberti et al., 2009). We applied current prion identification algorithms (Lancaster et al., 2014) to the proteins that induced the remaining nine Hsp104-dependent traits. They ranked among the lowest in the *S. cerevisiae* proteome (Table S3). These examples, which exceed the number of confirmed yeast prions (Garcia and Jarosz, 2014), establish the power of our approach to identify prion-like behaviors that have been missed in prior studies.

Alterations in Hsp70 and Hsp90 Activities Influence the Inheritance of Most Phenotypic States

The inheritance of one prion, [*GAR*$^{+}$], is Hsp104 independent. Instead, it can be heritably eliminated with transient inhibition of Hsp70, such as by expressing a dominant-negative variant (Ssa1-K69M; hereinafter, Hsp70^{DN}) (Brown and Lindquist, 2009; Jarosz et al., 2014b). We transformed strains harboring the remaining 35 Hsp104-independent states with a

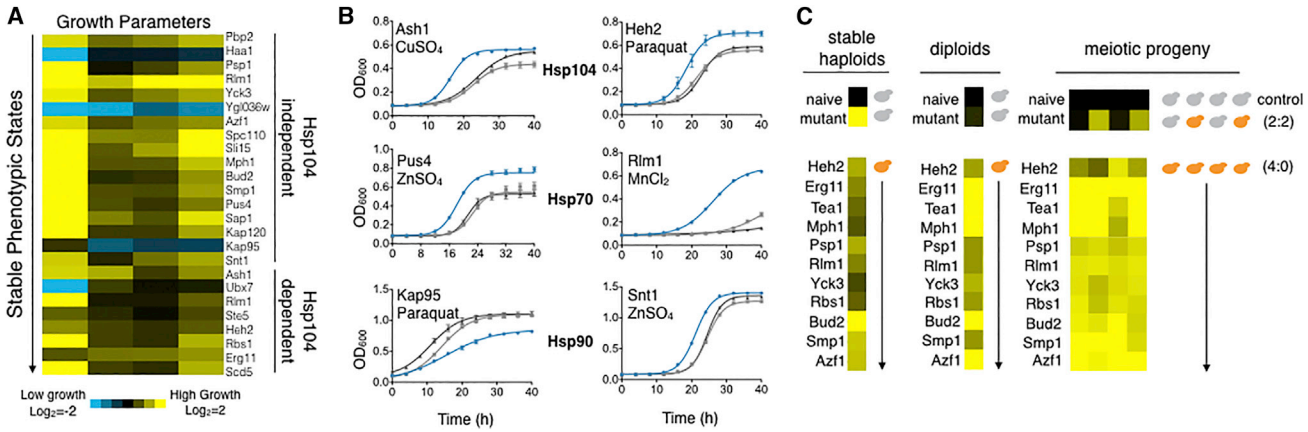

Figure 1. Transient Protein Overexpression Produces Stable Phenotypic States with Prion-like Patterns of Inheritance

(A) Growth parameters (in order: lag, slope, yield, and area under curve) in stress conditions for cells harboring stable phenotypic states relative to naive cells.

(B) Growth of cells harboring phenotypic states after curing by transient inhibition of Hsp104, Hsp70, and Hsp90. Error bars represent SE from three biological replicates. Blue indicates phenotypic state, dark gray indicates naive, and light gray indicates "cured." SE is ~15%. OD_{600}, optical density at 600 nm.

(C) Phenotypic states (orange) are dominant in genetic crosses to isogenic naive strains (gray) and exhibit non-Mendelian patterns of segregation (4:0 in tetrads). Segregation pattern of a spontaneous $ZnSO_4$-resistant mutant that arose during the screen is shown as a point of comparison (2:2 Mendelian inheritance rather than 4:0). Growth rates are shown in heatmap. SE is ~15%.

See also Figures S1 and S2.

plasmid that constitutively expressed $Hsp70^{DN}$, picked multiple transformants, and propagated them three times. We then eliminated the expression plasmid and grew the cells for ~25 generations on YPD to restore Hsp70 function. Many traits (19 of the 35) were eliminated by this regimen (Figure 1B; Figure S1C; Table S3; see Table S4 for genetic confirmation).

One other chaperone, Hsp90, has recently been implicated in a self-templating assembly mechanism underlying innate immunity (Hou et al., 2011) and in propagating a prion-like protein in plants (Chakrabortee et al., 2016). We tested whether it might influence any of the remaining 16 heritable phenotypic states by propagating strains harboring them four times in media containing radicicol, a potent Hsp90 inhibitor (Schulte et al., 1998). We then grew the strains for ~25 generations in standard medium to restore Hsp90 function. Two traits were heritably eliminated in these experiments (those elicited by Snt1 and Kap95; Figures 1A and 1B; Figure S1C; Table S3). Thus, in addition to other mechanisms by which Hsp90 can influence the inheritance of new traits (Jarosz et al., 2010), this chaperone also regulates prion-like inheritance. Protein homeostasis is achieved by the collective action of dozens of chaperones and co-chaperones. In at least two instances, prion inheritance requires other components of this network: propagation of [RNQ^+] requires the Hsp40 protein Sis1 (Aron et al., 2007; Sondheimer et al., 2001), and propagation of [*URE3*] is influenced by the co-chaperone Cpr7 (Kumar et al., 2015). Although beyond the scope of this work, other components of the protein homeostasis machinery may also influence the inheritance of the remaining 14 phenotypic states.

Protein-Induced Heritable Phenotypic States Act as Non-Mendelian Genetic Elements

We selected 18 heritable phenotypic states with different chaperone requirements to test for another defining characteristic of prion biology: non-Mendelian inheritance (Shorter and Lindquist, 2005). We crossed cells harboring these traits to naive, isogenic controls and tested how the traits segregated to meiotic progeny. Because fungal prions are not tied to the segregation of chromosomes, they are generally passed to most, if not all, meiotic progeny (4:0 or, occasionally, 3:1 inheritance in tetrads). In contrast, traits that arise from DNA mutations propagate to half of all progeny (2:2). For each of the proteins we examined, the crosses revealed strong a non-Mendelian pattern of inheritance (Figure 1C; Table S4).

A final defining feature of prions is cytoplasmic transmission (Shorter and Lindquist, 2005; Wickner et al., 2006). We mated donor strains harboring the heritable phenotypic states to *kar1-15* rho recipient strains (defective in nuclear fusion and mitochondrial respiration). We picked budding cells from the resulting heterokaryons, selecting those that bore genetic markers of the recipient strain but had received cytoplasm from the donor (scored by restored mitochondrial function). The stable phenotypic states were transferred to naive recipients through such cytoductions (Figures S2A and S2B). Control cytoductions with naive donors never produced these phenotypes. Because prion-based traits can depend on genetic background, we also performed a reverse cytoduction, using the recipients as donors and naive wild-type cells as recipients. The traits were also robustly transferred in these experiments. Given their non-Mendelian cytoplasmic inheritance and strong reliance on chaperone activity, we conclude that many of the heritable phenotypic states arise from prion-like mechanisms.

Traits Created by Protein-Based Inheritance Are Frequently Beneficial

Whether prion-based inheritance could provide adaptive benefit has been highly controversial (Byers and Jarosz, 2014). Many have argued that most prions represent pathological states (McGlinchey et al., 2011; Nakayashiki et al., 2005). Others have

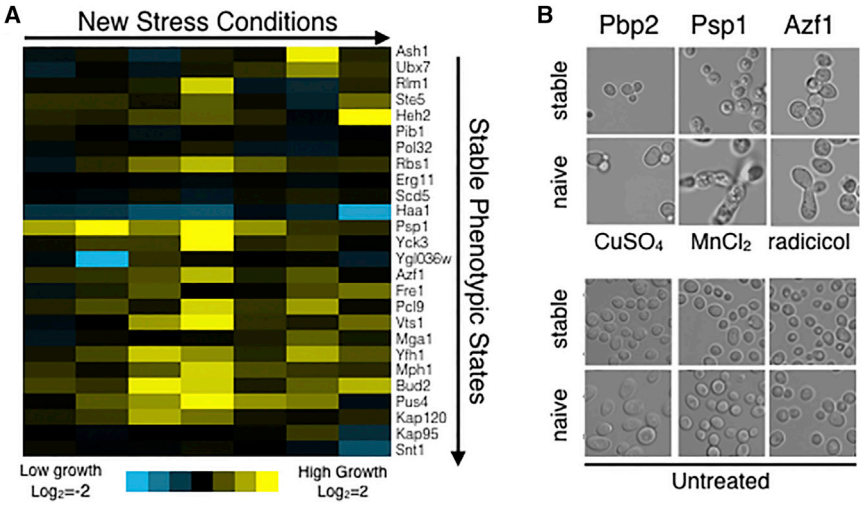

Figure 2. These Phenotypic States Encode Diverse Beneficial Traits

(A) Heatmap of growth rates for cells harboring the stable phenotypic states in no stress, osmotic stress (0.5 M NaCl), ethanol (5%), heat (39°C), acid stress (pH 4), basic stress (pH 9), and membrane stress (1 mM cetylpyridinium chloride). SE is ~15%.

(B) Micrographs (100× magnification) of cells harboring the indicated phenotypic states and naive cells.

suggested that fungal prions could serve as sophisticated bet-hedging devices that are beneficial in stressful environments (Griswold and Masel, 2009; Halfmann et al., 2012; Jarosz et al., 2014b; True and Lindquist, 2000). Most phenotypic states we identified were benign in rich medium and beneficial in the conditions we used to isolate them. We wondered whether they might also have adaptive value in other environments. Therefore, we challenged cells harboring the prion-like epigenetic states with six new stresses. Most were strikingly beneficial (Figure 2A). For example, the heritable epigenetic state created by transient overexpression of Psp1 increased growth rates 2-fold in osmotic stress (0.5 M NaCl) and by 50% in acidic stress (pH 4). Ten of the heritable phenotypic states provided measurable benefit in all the stress conditions we tested. Only one was more commonly detrimental than beneficial.

This biased distribution of fitness effects was often evident at the cellular level. Whereas naive cells exposed to the stressful conditions exhibited morphologies indicative of stress responses, those with prion-like epigenetic states were often indistinguishable from untreated cells. For example, naive cells exhibited an elongated morphology in $MnCl_2$, but those harboring the Psp1-induced prion-like state did not (Figure 2B). Collectively, our data establish that the prion-like states we have discovered are very commonly beneficial.

Protein-Based Phenotypic States Can Drive Gain of Function or Loss of Function

Many known prions mimic loss of function, presumably due to sequestration of the causal protein. However, for one prion-like protein, CPEB, the assembly serves as a scaffold for interacting proteins to regulate translation (Khan et al., 2015). Another protein, Het-s, acquires a novel function in the prion state (Seuring et al., 2012). We tested whether the traits we identified were due to gains or losses of function in the proteins that drove their appearance, comparing the cells harboring the prion-like epigenetic states to naive cells in which the corresponding inducing protein was deleted. These strains should have the same phenotypes if the trait was due to a loss of function.

Strains harboring the prion-like state created by transient overexpression of Smp1 had the same traits as Δ*smp1* strains. Smp1 is a transcriptional repressor. To investigate this protein-based phenotype at the molecular level, we measured expression of Smp1's target transcripts (e.g., *UBI4* and *TUF4*) with qPCR. We observed a similar degree of de-repression for these transcripts in cells harboring the prion-like state as in Δ*smp1* strains (Figure 3A). Indeed, among the 15 protein deletions that we tested in this way, seven phenocopied their protein's corresponding induced epigenetic state (those elicited by transient overexpression of Smp1, Mph1, Pus4, Psp1, Ygl036w, Haa1, and Sli15; Figure 3; Figure S3; Table S4). For brevity, we henceforth refer to these prion-like epigenetic states by the names of their inducing proteins (e.g., [*SMP1*$^+$]).

Four traits were more exaggerated than those produced by deletion of their inducing proteins (those elicited by transient overexpression of Azf1, Heh2, Pbp2, and Vts1; Figure 3; Figure S3; Table S4). Thus, they created phenotypes with a gain-of-function character. For example, the prion-like state created by transient overexpression of the Azf1 improved growth in radicicol even more than the *AZF1* deletion did (Figure 3B). Azf1 is a transcriptional activator. Therefore, we asked whether this heritable epigenetic state led to repression of Azf1-regulated transcripts (e.g., *MCH5* and *MDH2*). The reduction in transcript levels we measured by qPCR was greater than in *Δazf1* cells (Figure 3B).

Because Azf1 binds to DNA, it is possible that its overexpression created a conventional epigenetic state on chromatin that, once created, was stabilized by Azf1-independent means. To test whether Azf1 was required for the inheritance of this phenotypic state, rather than simply for its induction, we crossed cells harboring this state to naive Δ*azf1* cells. We sporulated the resulting diploids and isolated meiotic progeny. Progeny that inherited a functional *AZF1* gene inherited the trait, but those that inherited the *AZF1* deletion did not (Table S4). Therefore, we refer to this prion-like epigenetic state as [*AZF1*$^+$].

The remaining three heritable epigenetic states produced adaptive advantages unrelated to the deletion of their inducing proteins. For example, the state created by the Rlm1 transcription factor strongly improved growth in manganese, but *RLM1* deletion did not (Figure 3C). Expression of one Rlm1-regulated transcript, *RCK1*, was reduced in cells harboring the Rlm1-induced state but not in Δ*rlm1* cells. In contrast, expression of

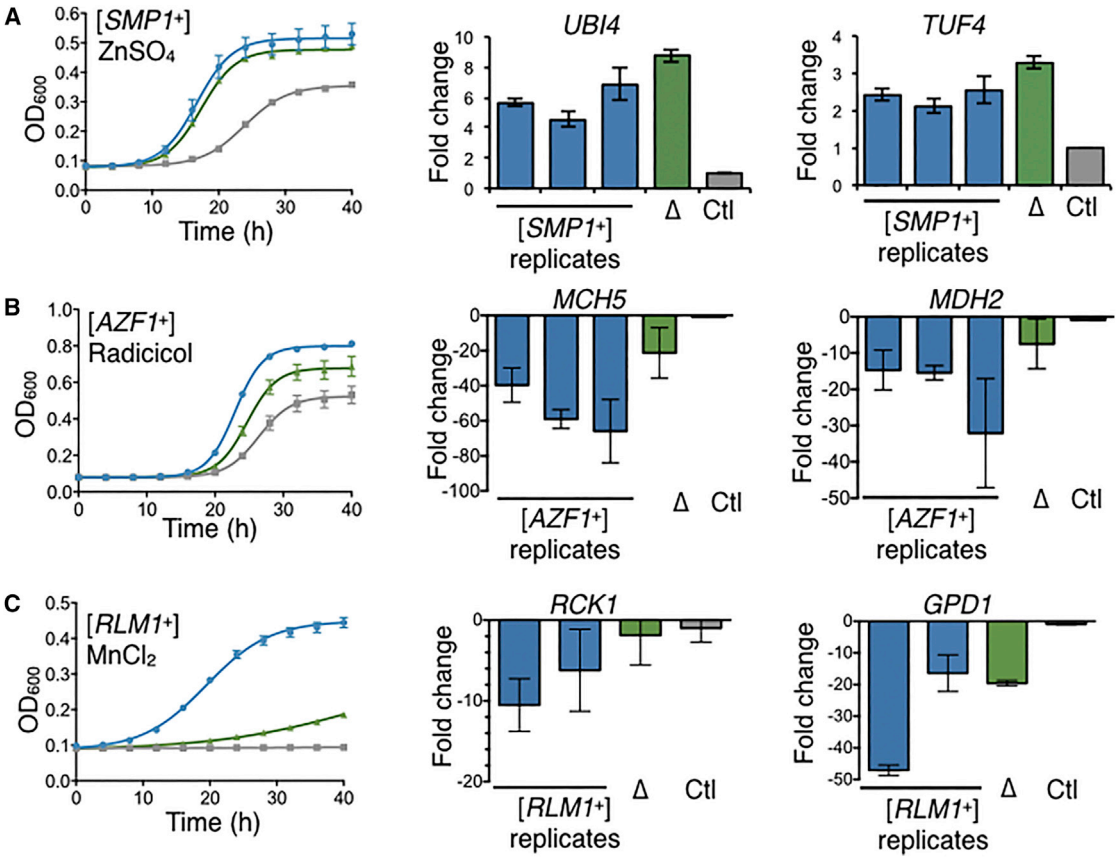

Figure 3. Prion-like Epigenetic Elements Encode Both Loss-of-Function and Gain-of-Function Traits

(A–C) Comparisons of growth phenotypes and gene expression patterns for strains harboring phenotypic states and strains in which their inducing proteins were deleted. Blue indicates strains harboring phenotypic states, green indicates deletions of inducing genes, and gray indicates naive controls (Ctl). Error bars represent SE from three biological replicates. OD_{600}, optical density at 600 nm.

See also Figure S3.

another Rlm1-regulated transcript, *GPD1*, was downregulated both in cells that harbored the phenotypic state and in Δ*rlm1* cells (Figure 3C). We tested whether Rlm1 was required for the continued inheritance of this state using a genetic-crossing strategy analogous to that we had used for [*AZF1*$^+$]. Meiotic progeny that inherited a functional *RLM1* gene inherited the epigenetic state. Those that inherited the *RLM1* deletion did not (Table S4). Thus, Rlm1 protein is essential for the maintenance of this phenotypic state, which we hereinafter refer to as [*RLM1*$^+$]. We examined five additional prion-like states analogously to determine whether the proteins that induced them were also responsible for their maintenance. Three of them were. For brevity, we also refer to these states as [*PSP1*$^+$], [*VTS1*$^+$], and [*RBS1*$^+$] (Table S4). The relationship between the remaining four phenotypes and the proteins that induce them remains unclear.

Inducing Proteins Do Not Commonly Form Amyloid Fibers

Domains from a handful of inducing proteins were previously tested for their ability to form amyloids because of their amino-acid sequence bias (Alberti et al., 2009). Only one did (Rbs1). Because our data established that all could, nonetheless, act as prion-like elements, we investigated their biochemical and cell biological characteristics. We took advantage of an *S. cerevisiae* library in which each ORF has been endogenously tagged with GFP at its C terminus (Ghaemmaghami et al., 2003). We crossed cells harboring eight representative prion-like states to cells expressing GFP-tagged variants of their inducing proteins. As a negative control, we crossed these same ORF-GFP strains to isogenic naive cells.

Amyloid assemblies can be separated by semi-denaturing detergent-agarose gel electrophoresis (SDD-AGE): amyloid fibers migrate in the high-molecular-weight (HMW) fraction, whereas soluble protein migrates more rapidly. None of the diploids showed a signal in the HMW amyloid fraction of SDD-AGE blots (Figure 4A; 18-hr exposure), in contrast to lysates from cells harboring [*PSI*$^+$] (Figure 4A; 10-min exposure). Importantly, we did not observe cross-seeding with other prion proteins (Figure S4A).

Next, we examined the localization of the GFP fusion proteins in diploids harboring the prion-like states. None displayed the large fluorescent foci characteristic of canonical yeast prions. However, many had altered signal or localization compared to naive controls (Figure 4B). Because the levels of inducing protein

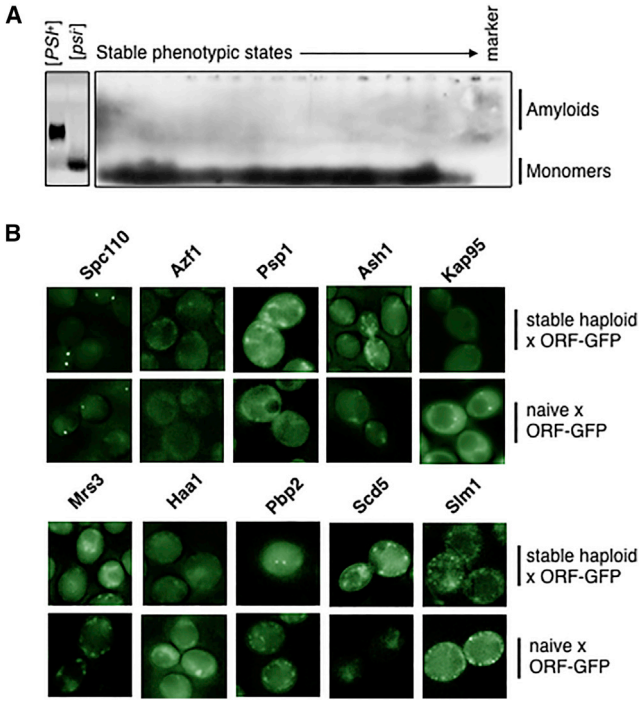

Figure 4. Proteins that Induce Phenotypic States Do Not Form Amyloid Fibers

(A) Immunoblot of SDD-AGE run of lysates from diploid cells harboring stable phenotypic states and expressing integrated GFP-tagged copies of their inducing proteins at 18 hr exposure. [*PSI*$^+$] shows robust signal (at 30 min exposure). The first three lanes of the blot contain three independent isolates of the [*PSP1*$^+$] prion, followed by [*psp1*$^-$], [*SPC110*$^+$], [*spc110*$^-$], [*HAA1*$^+$], [*haa1*$^-$], [*HEH2*$^+$], [*heh2*$^-$], [*BUD2*$^+$], [*bud2*$^-$], [*RBS1*$^+$], [*rbs1*$^-$], [*VTS1*$^+$], [*vts1*$^-$], [*MPH1*$^+$], and [*mph1*$^-$].

(B) Representative fluorescence micrographs from similarly constructed diploids.

See also Figures S4 and S7.

were similar in these cells (when it could be detected by immunoblot; Figure S4B), these differences likely reflect an altered chemical environment for the fluorophore, driven by the associated protein-based phenotypic states. Although the structure of these elements remains to be defined, our data establish that non-amyloid conformational states may serve as a common means for catalyzing protein-based inheritance.

This Type of Inheritance Arises in Nature

We previously reported that Hsp104-dependent prions are common in wild fungi (Halfmann et al., 2012). Therefore, we investigated whether protein-based traits of the type that we have discovered here—Hsp104 independent but sensitive to Hsp70 and Hsp90 perturbation—were also present in nature. We transiently inhibited each chaperone (as described earlier in the text) in four biological replicates of more than 2 dozen wild *S. cerevisiae* isolates (from diverse ecotypes; see Table S5). We propagated the same parental wild yeast isolates on YPD alone for an equivalent number of generations to control for changes in phenotype that might arise from serial passage.

Transient chaperone inhibition sparked an extraordinary degree of heritable phenotypic diversification in these strains (Figure 5A). The traits were reproducible and both strain and chaperone specific, establishing that they were not merely caused by general phenotypic instability. For example, strain YB-210 (a fruit isolate) grew poorly in the presence of the cell wall toxin calcofluor white, but grew robustly after transient inhibition of Hsp70. Transient inhibition of Hsp104 and Hsp90 had no effect on this trait. Strain Y-584 (a wine isolate) was resistant to the DNA replication stressor hydroxyurea. This trait was lost following the transient inhibition of Hsp90 but was not strongly affected by transient inhibition of either Hsp70 or Hsp104. In other cases, different chaperone perturbations had opposing effects. For example, the Belgian Strong Ale strain Wyeast 1388 was modestly resistant to ethanol, and transient inhibition of Hsp70 heritably enhanced this trait. In contrast, transient inhibition of Hsp90 eliminated it. In addition to growth traits, we also commonly observed changes in colony morphology that had similar, chaperone-dependent patterns of inheritance (Figure 5B).

We also constructed a reporter for [*MPH1*$^+$] and used it to measure spontaneous gain and loss of this Hsp104-independent epigenetic state. We first compared the transcriptomes of [*MPH1*$^+$] and [*mph1*$^-$] cells by RNA sequencing. As expected, given that Mph1 is not a known regulator of gene expression, only a single transcript was significantly affected (*MDG1*, which encodes a protein with a minor role in pheromone signaling, was downregulated 3-fold; Bonferroni-corrected $p = 0.037$). We replaced this gene with a counter-selectable *URA3* marker. Naive [*mph1*$^-$] cells harboring this reporter grew on synthetic defined media lacking uracil (SD-URA) but not on counter-selective media containing 5-fluoroorotic acid (5-FOA). In contrast, [*MPH1*$^+$] cells grew poorly on media lacking uracil but grew well on media containing 5-FOA ([*MPH1*$^+$] cells did grow on SD-URA after 7 days, consistent with the modest degree of *MDG1* repression; Figure S5).

Next, we plated [*mph1*$^-$] cells harboring the reporter on media containing 5-FOA. The frequency at which colonies arose, $4.0 (\pm 1.0) \times 10^{-7}$, was higher than would be expected from mutation ($\sim 5.43 \times 10^{-8}$; Lang and Murray, 2008). Moreover, most colonies (64 of 87 were tested) also manifested the original phenotype of [*MPH1*$^+$] (dominant resistance to zinc sulfate; see Supplemental Information for further discussion). Next, we used the reporter to examine [*MPH1*$^+$] loss, plating saturated cultures of [*MPH1*$^+$] cells onto media lacking uracil. The frequency with which URA+ colonies appeared, $1.2 (\pm 0.6) \times 10^{-6}$, was also higher than would be expected from mutation alone. These data establish that the heritable protein-based phenotypic states we have discovered here can be acquired and lost spontaneously, in the absence of overexpression, and have the power to exert a strong influence on phenotypic inheritance in nature.

Phenotypic States Are Driven by Transmittable Protein-Based Genetic Elements

The "gold-standard" test for prion-based inheritance is heritable transformation of naive cells with protein alone (Tanaka et al., 2004; Wang et al., 2010). Making no assumptions about the

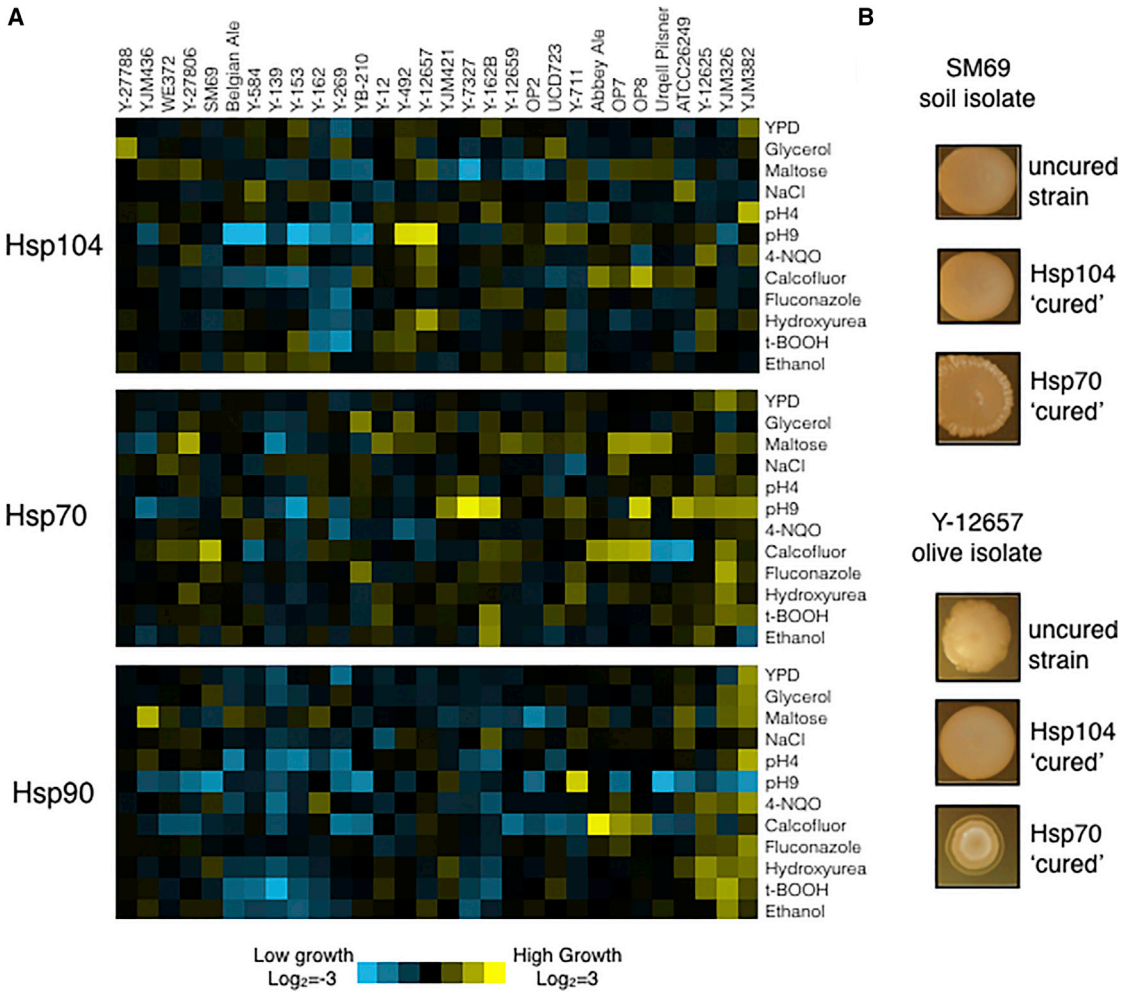

Figure 5. Wild Yeast Strains Harbor Hsp104-Independent Phenotypic States

(A) Heritable changes in growth rate of wild *S. cerevisiae* isolates elicited by transient inhibition of Hsp104, Hsp70, and Hsp90. The average change in growth rate from four biological replicates is plotted. SE is ~20%. Strains are clustered by similarity in phenotype upon Hsp104 curing.

(B) Colony morphology phenotypes of wild strains grown on 0.5% YPD agar for 7 days at 30°C after transient chaperone curing.

See also Figure S5.

causal proteins' stoichiometry, post-translational modifications, or participation in multi-protein complexes, we used nuclease-digested lysates for these experiments (Figure 6A). First, we grew naive cells and cells harboring [*AZF1*$^+$], [*RLM1*$^+$], and [*PSP1*$^+$] to mid-exponential phase. Next, we enzymatically removed their cell walls, generating spheroplasts. We sonicated the spheroplasts, spun down the cell debris, and eliminated nucleic acid from the lysates by over-digestion with RNase and DNase (subsequently recovering the enzyme by affinity purification; see Supplemental Information). We transformed naive spheroplasts with these nuclease-treated lysates, including a carrier plasmid containing *URA3* as a control for transformation. We then picked dozens of URA+ colonies from each transformation, selected for loss of the carrier plasmid on 5-FOA, and characterized the phenotypes of the resulting cells.

The efficiency of these transformations was remarkable (Figure 6B; Table S6). 53% of the cells transformed with [*PSP1*$^+$] lysates acquired the [*PSP1*$^+$] phenotype (resistance to $MnCl_2$; $p = 7 \times 10^{-4}$ by t test); 48% of the cells that were transformed with [*AZF1*$^+$] lysates acquired the [*AZF1*$^+$] phenotype (resistance to radicicol; Figure 4A; $p = 10^{-12}$ by t test); 50% of the cells that were transformed with [*RLM1*$^+$] lysates from the cells acquired the [*RLM1*$^+$] phenotype (resistance to $MnCl_2$; $p = 10^{-3}$ by t test). Cells that were transformed with [*prion*$^-$] lysates did not display [*PRION*$^+$] phenotypes. This efficiency is extraordinarily high, given the low expression levels of these proteins – ~50 molecules per cell for Azf1 and Rlm1; ~340 molecules per cell for Psp1 (Chong et al., 2015; Kulak et al., 2014; Nagaraj et al., 2012). When benchmarked against [*PSI*$^+$], these phenotypic states are 20–70 times more "infectious" (Table S6). Thus, the Hsp104-independent "memories" we have discovered can act as bona fide prions and comprise a remarkably robust family of protein-based genetic elements.

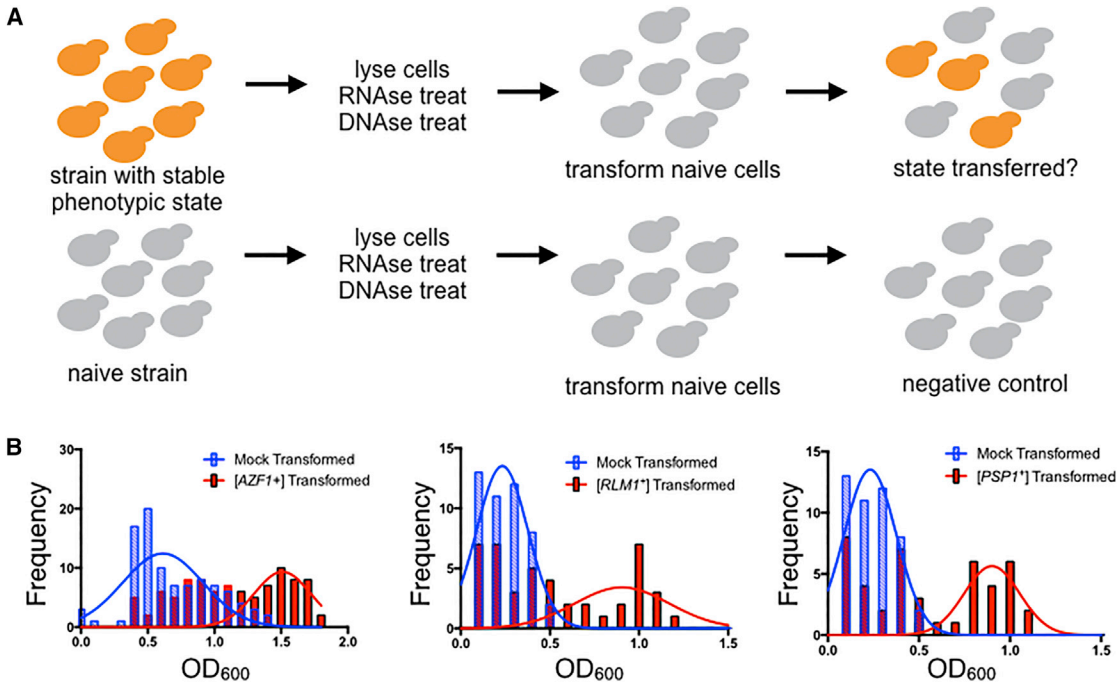

Figure 6. Transmissibility of Stable Epigenetic States by Protein Alone

(A) Experimental schema.

(B) Histogram showing growth for [*HEH2*$^+$], [*AZF1*$^+$], [*PSP1*$^+$] and [*RLM1*$^+$] transformants. Blue bars indicate transformants from incubations with lysates derived from naive cells. Red bars indicate transformants from incubations with lysates derived from cells harboring the indicated phenotypic state. The naive distribution was fit with a Gaussian and used to threshold transformations that were successful, which were then fit to a separate Gaussian distribution. OD_{600}, optical density at 600 nm.

Inducing Proteins Harbor Regions of Extreme Disorder

Only a handful of inducing proteins had Q/N-rich sequences and established algorithms did not identify the majority as "prion-like" (Table S3; Figure S6A). The hits did have a slight enrichment in serine content (10.7 ± 2.8% versus 8.8 ± 3.8% for the yeast proteome; Figure S6A; $p = 0.006$ by t test) but did not commonly harbor low-complexity sequences. However, the inducing proteins had a striking enrichment in intrinsically disordered sequences using Disopred3 (Jones and Cozzetto, 2015) and several other prediction algorithms (see Supplemental Information; $p < 0.0001$ relative to the proteome; Figure 7A). Most disordered regions of sequence were punctuated by smaller ordered regions that often contained the proteins' functional domains (Figure 7B).

We wondered whether the intrinsically disordered regions (IDRs) in the inducing proteins we discovered might have an function analogous to that of the modular Q/N rich sequences in canonical prions. We examined this possibility for Psp1, which has a very clearly demarcated IDR (Figure S6B). In naive wild-type cells, we transiently induced full-length Psp1, Psp1's IDR alone, and a Psp1 variant lacking its IDR. We tested whether these constructs could elicit the expected phenotypic state: [*PSP1*$^+$]-dependent manganese resistance. Transient overexpression of full-length Psp1 and its IDR alone did so robustly, although the magnitude of the phenotype was slightly larger for the full-length protein (Figures S6B and S6C). In contrast, the Psp1 variant lacking its IDR did not induce the phenotypic states.

Conservation of Disorder and the Capacity to Fuel Protein-Based Inheritance

To investigate the evolutionary conservation of these patterns of interspersed order and disorder, we identified orthologs of inducing proteins from fungi that diverged from *S. cerevisiae* between 5 million and 200 million years ago (Wapinski et al., 2007). As a frame of reference, 100 million years is enough time for every nucleotide in the genome to have been permuted at least twice (Langkjaer et al., 2003). We then performed disorder predictions for these orthologs. Despite considerable sequence divergence, we observed remarkable conservation of long regions of intrinsic disorder. This feature is shared even by several known N/Q-rich prions. However, the hits from our screen were unusual in that the alternating patterns of order and disorder were conserved in fine detail, despite considerable sequence divergence (Figure 7B). This so-called "flexible disorder" has been identified computationally in proteins involved in cell-cycle control, signal transduction, and other forms of biological regulation (Bellay et al., 2011).

We investigated whether these conserved patterns of disorder (Figure S6D) were linked to the retention of prion-like behavior in the human homologs of our hit proteins. We investigated the capacity of three to seed the formation of a heritable, altered physical state (Figure 7C). We transformed yeast cells with GFP-tagged variants of Ipo11 (homolog of Kap120), Pold3 (homolog of Pol32), and Mef2d (homolog of Rlm1) under the control of an inducible galactose promoter. Then,

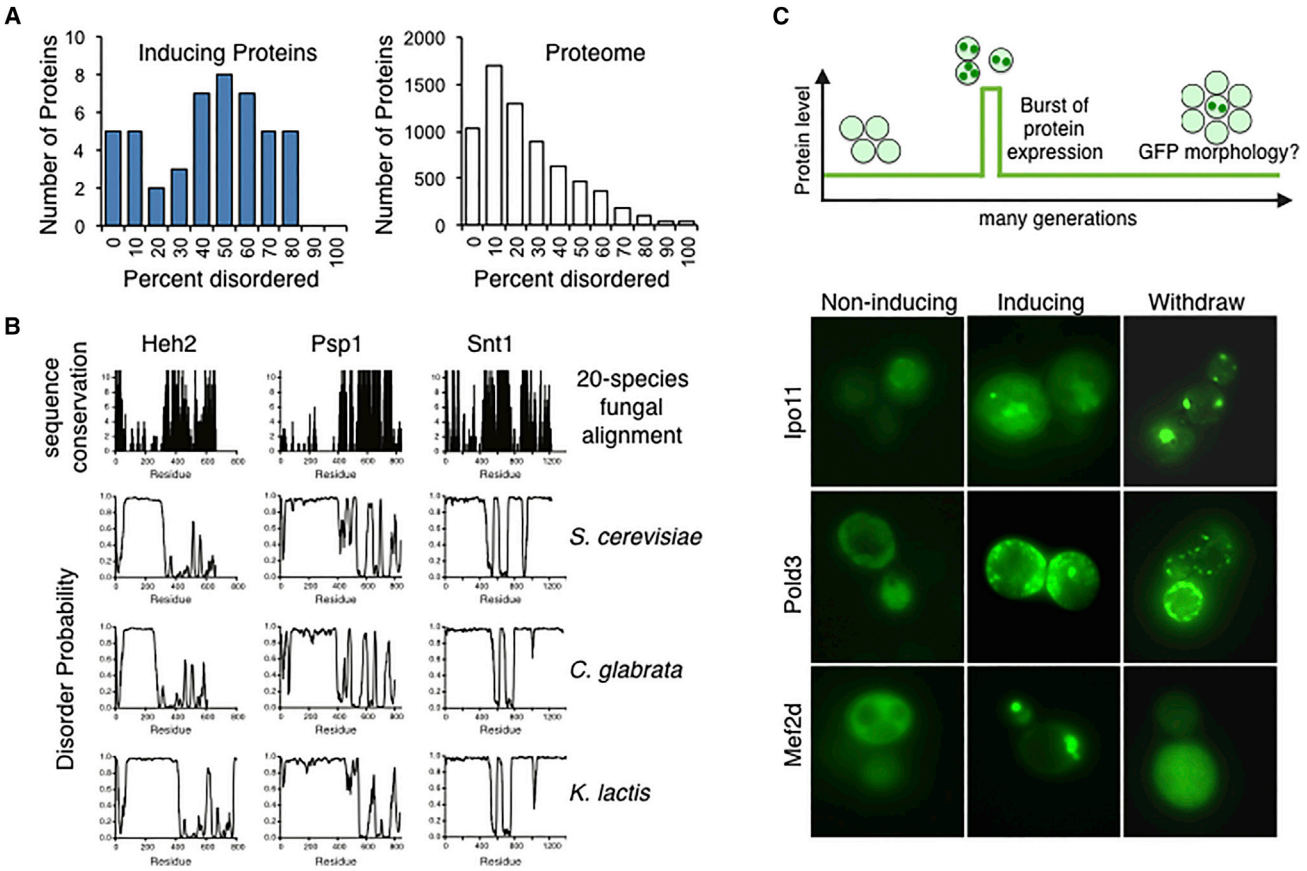

Figure 7. Proteins that Induce Protein-Based Inheritance Are Enriched in Intrinsically Disordered Sequences

(A) Disorder scores of inducing proteins relative to the *S. cerevisiae* proteome.

(B) Long segments of predicted disorder maintained over great evolutionary distances without underlying sequence conservation. Conservation scores (0–11) were calculated with an ~20 species alignment of the *Saccharomyces* complex (see Supplemental Information). Conservation scores calculated with respect to *S. cerevisiae* sequence.

(C) Top: schema for seeding experiments. Typical protein aggregates formed upon overexpression should dissipate after the overexpression is stopped and upon further growth, dependent on dilution. Bottom: seeding behavior of three human homologs of inducing proteins with conserved intrinsic disorder. The GFP-tagged proteins are diffuse but aggregate when overexpressed. After dilution back into low-expression conditions and outgrowth, two proteins retained their altered morphology (35%–40% versus < < 1% expectation frequency; see Figure S6D).

See also Figure S6.

we examined their localization patterns under low-expression conditions (media with raffinose or very low concentrations of galactose). All three had a diffuse distribution that was maintained for hundreds of generations (Figure 7C). We then overproduced these proteins for 8 hr in 2% galactose. This caused each of the proteins to form fluorescent foci. To test whether this state would be maintained in progeny that were not overexpressing the protein, we diluted the cells 200-fold and grew them to saturation for 48 hr in low-expression conditions. One of the proteins, Mef2d, returned to the diffuse state. The other two, Ipo11 and Pold3, propagated as foci in the progeny (Figure 7C; Figures S6E and S7). Because of the large dilution factor we used, and an experimental timescale that vastly exceeded the average half-life of human proteins, we conclude that, for at least some of the inducing proteins, the capacity to adopt a heritable, altered molecular state has been conserved from yeast to man.

DISCUSSION

Protein-based inheritance has long been considered a paradigm-shifting, but rare, means of biological information transfer. We have found that this is far from true: many eukaryotic proteins have the capacity to encode heritable phenotypic states. These states share the same unusual patterns of inheritance as prions, yet all but one that we discovered are not known prions. Instead, they are enriched in transcription factors and RNA-binding proteins that harbor distinctive patterns of interspersed ordered and disordered sequences. This physiochemical property has been widely conserved across evolution, along with the capacity of some orthologous proteins to transmit phenotypic states. Traits produced by this mode of inheritance are strikingly beneficial and are common in wild yeast. Our data collectively establish that protein-based inheritance is much more pervasive than had previously been suspected and that

it has the capacity to broadly influence the emergence of adaptive traits.

The self-templating conformations of prion proteins uncouple genotype from phenotype. This allows genetically identical cells in a population to acquire new phenotypes and can provide strong adaptive advantages in stressful environments (Byers and Jarosz, 2014). Most prions have been identified based on low-complexity sequence biases and the capacity to adopt amyloid conformations. The prions we discovered here do not share those properties. Instead, they resemble a hitherto unique prion-like element that confers extraordinary adaptive value and alters metabolic dynamics in microbial communities (Brown and Lindquist, 2009; Jarosz et al., 2014a, 2014b). This element, [*GAR*$^+$], is strongly induced by environmental stimuli, most notably, cross-kingdom chemical communication with bacteria (Jarosz et al., 2014a). However, the nearly 50 prion-like states of this type that we discovered are likely to be just the tip of the iceberg: the phenotypic landscape in this screen is limited both by the number of conditions we used and by the efficiency of prion induction. Indeed, several known prions would not be induced to a sufficient extent for us to have recovered them. Thus, the breadth of protein-based inheritance is almost certainly more extensive that what we have discovered here.

Although the protein-based phenotypic states we discovered share the genetic features of prions, their mechanisms of propagation are strikingly different. Most are Hsp104 independent. Instead, their transmission was commonly blocked by transient inhibition of either Hsp70 or Hsp90. This degree of Hsp104 independence has only previously been observed for a handful of protein-based "molecular memories," such as the Whi3 mnemon (Caudron and Barral, 2013) and [*GAR*$^+$] (Brown and Lindquist, 2009). Additional studies are needed to elucidate the structural basis for their propagation, but our results strongly suggest that non-amyloid structures can commonly fuel protein-based inheritance. Our findings thus establish that [*GAR*$^+$] is far from unique and, instead, is the founding member of what may be a very large class of protein-based genetic elements. [*GAR*$^+$] has the unusual ability to undergo wholesale induction and loss in an entire population of cells in response to specific environmental stimuli (Jarosz et al., 2014a; Tapia and Koshland, 2014). Thus, in addition to acting as bet-hedging devices, the non-amyloid conformations that drive these phenotypic states could, in principle, permit dynamic switch-like induction and loss in response to specific environmental cues.

These phenotypic states also pass the gold-standard test for protein-based inheritance—cellular transformation by protein alone—establishing their robust nature. This test has been used both for canonical yeast prions, such as [*PSI*$^+$] (Tanaka et al., 2004), and more broadly through injection of "prion-like" fibers of some neurodegenerative disease proteins directly into animals (Peelaerts et al., 2015). These experiments succeeded with extremely abundant proteins or in sensitized backgrounds where the proteins were constitutively overproduced. When benchmarked against their low intracellular abundance, the protein-based genetic elements we have discovered are orders of magnitude more infectious than other prions. In vivo, [*PSI*$^+$] cannot be induced at all unless another prion ([*PIN*$^+$]) is also present (Derkatch et al., 2001; Sondheimer and Lindquist, 2000), although it can be transmitted to [*pin*$^-$] strains with protein transformation (Tanaka et al., 2004). The robust transformation efficiencies, and induction efficiencies, of the prion-like states that we discovered provides an explanation for the reproducibility with which they were elicited by transient overexpression.

Prions such as [*PSI*$^+$] (True and Lindquist, 2000), [*MOD*$^+$] (Suzuki et al., 2012), or [*GAR*$^+$] (Brown and Lindquist, 2009; Jarosz et al., 2014a, 2014b) can be strikingly beneficial in some conditions but are detrimental in others. Many lines of evidence support the potential adaptive value of these prions as bet-hedging elements owing to their occasional, but strong, fitness benefits (Griswold and Masel, 2009; Jarosz et al., 2014b; True and Lindquist, 2000). Even against this backdrop, the phenotypic states we have discovered here have strong adaptive potential. Together with the many beneficial Hsp104-dependent traits previously observed in laboratory and wild strains (Halfmann et al., 2012; True and Lindquist, 2000), these new prion-like elements comprise a large reservoir of heritable phenotypic diversity that could empower the ability of natural yeast populations to thrive fluctuating environments.

Prions often sequester proteins away from their normal cellular functions (Shorter and Lindquist, 2005; Wickner et al., 2006), with a handful of exceptions (Khan et al., 2015; Seuring et al., 2012). Here, we observed that only about half of the phenotypic states mimicked loss of function of their inducing protein. The remainder produced gains of function. In some cases, these were exaggerated dominant-negative phenotypes, and in other cases, they were completely unrelated to the known phenotypes of the inducing protein. Both behaviors drove immediate sampling of diverse adaptive traits. The strong enrichment among inducing proteins for transcriptional and post-transcriptional regulators suggest that heritable remodeling of gene expression patterns might commonly drive these traits. Indeed, the fact that at least 10% of yeast transcription factors have this property may portend a broad role for protein-based inheritance of this type in stress responses and developmental processes.

Nearly 30% of the heritable protein-based epigenetic states we discovered were not affected by the perturbations in the chaperone activity that we used. The very strong reproducibility with which they arose established that they were not random mutations. In principle, these could be prions that rely on other arms of the protein homeostasis network to propagate. However, other types of phenotypic bistability can also produce phenotypic memories (Greer et al., 2011; Ozbudak et al., 2004; Rechavi et al., 2011). Indeed, such behavior has previously been engineered into an enzymatic reaction to produce a synthetic prion-like state (Roberts and Wickner, 2003). These mechanisms generally persist over a small number of generations and are not known to be transmittable by protein transformation, but they could, in principle, also be stabilized to fuel trans-generational epigenetic inheritance.

In the past decade, several broad functions have been attributed to intrinsically disordered proteins (IDPs) (Wu and Fuxreiter, 2016), including regulation of transcription and signal transduction, acting molecular shields to provide desiccation tolerance, and even promoting enzymatic activity. Perhaps as a consequence of this functional promiscuity, IDPs are also associated

with human disease (Uversky et al., 2009) and with dosage sensitivity in yeast, flies, and worms (Vavouri et al., 2009). Our results establish another widespread and evolutionarily conserved role for IDPs: the initiation and maintenance of protein-based inheritance. The features that drive intrinsic disorder in the proteins we identified are common across eukaryotic proteomes, including in humans, where N/Q-rich sequences are rare. Indeed, several human homologs of the inducing proteins retain the capacity to initiate and maintain heritable assemblies. Thus, our findings greatly expand the scope and evolutionary breadth of protein-based inheritance and suggest that it may be broadly used across eukaryotes to induce heritable epigenetic switches that transform phenotypic landscapes and drive adaptation to stressful environments.

STAR★METHODS

Detailed methods are provided in the online version of this paper and include the following:

- KEY RESOURCES TABLE
- CONTACT FOR REAGENT AND RESOURCE SHARING
- EXPERIMENTAL MODEL AND SUBJECT DETAILS
- METHOD DETAILS
  - Yeast Techniques
  - Phenotypic assays
  - Gene Expression Measurements
  - Computational Analyses
  - Aggregation Assays
  - Microscopy
  - Seeding assays for human orthologs
  - Lysate Transformations
- QUANTIFICATION AND STATISTICAL ANALYSIS

SUPPLEMENTAL INFORMATION

Supplemental Information includes seven figures and six tables and can be found with this article online at http://dx.doi.org/10.1016/j.cell.2016.09.017.

AUTHOR CONTRIBUTIONS

S.C., J.S.B., S.L., and D.F.J. designed the experiments. D.F.J., S.C., J.S.B., S.J., B.B., A.C., L.L., D.M.G., R.S., and B.F. carried out the original phenotypic screen; follow-up physiological, genetic, cell biological, and biochemical characterizations and analyzed the data. S.C., J.S.B., S.L., and D.F.J. wrote the paper.

ACKNOWLEDGMENTS

We thank J. Brown, E. Yeger-Lotem, K. Frederick, and L. Li, along with members of the S.L. and D.F.J. laboratories for materials, discussions, and comments. This work was supported by an NIH Pathway to Independence Award (R00-GM098600) and NIH New Innovator Award (NIH-DP2-GM119140) to D.F.J. D.F.J. was also supported as a Searle Scholar (14-SSP-210) and Kimmel Scholar (SKF-15-154) and by the David and Lucile Packard Foundation. This work was also funded by grants from the Harold and Leila Mathers Charitable Foundation and the Eleanor Schwartz Charitable Foundation to S.L. S.L. is a Howard HHMI investigator. S.C. was supported by a Broodbank Fellowship and as a Former Fellow of Hughes Hall, University of Cambridge. J.S.B. was supported by NIH training grant T32-GM007790, and D.M.G. was supported by postdoctoral fellowships from the Ford Foundation and the NIH (F32-GM109680).

Received: January 28, 2016
Revised: June 17, 2016
Accepted: September 7, 2016
Published: September 29, 2016

REFERENCES

Alberti, S., Gitler, A.D., and Lindquist, S. (2007). A suite of Gateway cloning vectors for high-throughput genetic analysis in *Saccharomyces cerevisiae*. Yeast *24*, 913–919.

Alberti, S., Halfmann, R., King, O., Kapila, A., and Lindquist, S. (2009). A systematic survey identifies prions and illuminates sequence features of prionogenic proteins. Cell *137*, 146–158.

Alberti, S., Halfmann, R., and Lindquist, S. (2010). Biochemical, cell biological, and genetic assays to analyze amyloid and prion aggregation in yeast. Methods Enzymol. *470*, 709–734.

Aron, R., Higurashi, T., Sahi, C., and Craig, E.A. (2007). J-protein co-chaperone Sis1 required for generation of [RNQ+] seeds necessary for prion propagation. EMBO J. *26*, 3794–3803.

Balbirnie, M., Grothe, R., and Eisenberg, D.S. (2001). An amyloid-forming peptide from the yeast prion Sup35 reveals a dehydrated beta-sheet structure for amyloid. Proc. Natl. Acad. Sci. USA *98*, 2375–2380.

Bellay, J., Han, S., Michaut, M., Kim, T., Costanzo, M., Andrews, B.J., Boone, C., Bader, G.D., Myers, C.L., and Kim, P.M. (2011). Bringing order to protein disorder through comparative genomics and genetic interactions. Genome Biol. *12*, R14.

Belle, A., Tanay, A., Bitincka, L., Shamir, R., and O'Shea, E.K. (2006). Quantification of protein half-lives in the budding yeast proteome. Proc. Natl. Acad. Sci. USA *103*, 13004–13009.

Boyé-Harnasch, M., and Cullin, C. (2006). A novel in vitro filter trap assay identifies tannic acid as an amyloid aggregation inducer for HET-s. J. Biotechnol. *125*, 222–230.

Brachmann, C.B., Davies, A., Cost, G.J., Caputo, E., Li, J., Hieter, P., and Boeke, J.D. (1998). Designer deletion strains derived from Saccharomyces cerevisiae S288C: a useful set of strains and plasmids for PCR-mediated gene disruption and other applications. Yeast *14*, 115–132.

Brown, J.C., and Lindquist, S. (2009). A heritable switch in carbon source utilization driven by an unusual yeast prion. Genes Dev. *23*, 2320–2332.

Byers, J.S., and Jarosz, D.F. (2014). Pernicious pathogens or expedient elements of inheritance: the significance of yeast prions. PLoS Pathog. *10*, e1003992.

Caudron, F., and Barral, Y. (2013). A super-assembly of Whi3 encodes memory of deceptive encounters by single cells during yeast courtship. Cell *155*, 1244–1257.

Chakrabortee, S., Kayatekin, C., Newby, G.A., Mendillo, M.L., Lancaster, A., and Lindquist, S. (2016). Luminidependens (LD) is an Arabidopsis protein with prion behavior. Proc. Natl. Acad. Sci. USA *113*, 6065–6070.

Chernoff, Y.O., Lindquist, S.L., Ono, B., Inge-Vechtomov, S.G., and Liebman, S.W. (1995). Role of the chaperone protein Hsp104 in propagation of the yeast prion-like factor [psi+]. Science *268*, 880–884.

Chong, Y.T., Koh, J.L., Friesen, H., Duffy, S.K., Cox, M.J., Moses, A., Moffat, J., Boone, C., and Andrews, B.J. (2015). Yeast proteome dynamics from single cell imaging and automated analysis. Cell *161*, 1413–1424.

Collart, M.A., and Oliviero, S. (2001). Preparation of yeast RNA. In Current Protocols in Molecular Biology, *Chapter 13*, Ausubel F.M., ed. (Wiley), Unit 13.12.

Conde, J., and Fink, G.R. (1976). A mutant of Saccharomyces cerevisiae defective for nuclear fusion. Proc. Natl. Acad. Sci. USA *73*, 3651–3655.

Coustou, V., Deleu, C., Saupe, S., and Begueret, J. (1997). The protein product of the het-s heterokaryon incompatibility gene of the fungus Podospora anserina behaves as a prion analog. Proc. Natl. Acad. Sci. USA *94*, 9773–9778.

Derkatch, I.L., Chernoff, Y.O., Kushnirov, V.V., Inge-Vechtomov, S.G., and Liebman, S.W. (1996). Genesis and variability of [PSI] prion factors in Saccharomyces cerevisiae. Genetics *144*, 1375–1386.

Derkatch, I.L., Bradley, M.E., Hong, J.Y., and Liebman, S.W. (2001). Prions affect the appearance of other prions: the story of [PIN(+)]. Cell *106*, 171–182.

Du, Z., Crow, E.T., Kang, H.S., and Li, L. (2010). Distinct subregions of Swi1 manifest striking differences in prion transmission and SWI/SNF function. Mol. Cell. Biol. *30*, 4644–4655.

Ferreira, P.C., Ness, F., Edwards, S.R., Cox, B.S., and Tuite, M.F. (2001). The elimination of the yeast [PSI+] prion by guanidine hydrochloride is the result of Hsp104 inactivation. Mol. Microbiol. *40*, 1357–1369.

Garcia, D.M., and Jarosz, D.F. (2014). Rebels with a cause: molecular features and physiological consequences of yeast prions. FEMS Yeast Res. *14*, 136–147.

Ghaemmaghami, S., Huh, W.K., Bower, K., Howson, R.W., Belle, A., Dephoure, N., O'Shea, E.K., and Weissman, J.S. (2003). Global analysis of protein expression in yeast. Nature *425*, 737–741.

Gietz, D., St. Jean, A., Woods, R.A., and Schiestl, R.H. (1992). Improved method for high efficiency transformation of intact yeast cells. Nucleic Acids Res. *20*, 1425.

Glover, J.R., Kowal, A.S., Schirmer, E.C., Patino, M.M., Liu, J.J., and Lindquist, S. (1997). Self-seeded fibers formed by Sup35, the protein determinant of [PSI+], a heritable prion-like factor of S. cerevisiae. Cell *89*, 811–819.

Greer, E.L., Maures, T.J., Ucar, D., Hauswirth, A.G., Mancini, E., Lim, J.P., Benayoun, B.A., Shi, Y., and Brunet, A. (2011). Transgenerational epigenetic inheritance of longevity in Caenorhabditis elegans. Nature *479*, 365–371.

Griswold, C.K., and Masel, J. (2009). Complex adaptations can drive the evolution of the capacitor [PSI], even with realistic rates of yeast sex. PLoS Genet. *5*, e1000517.

Halfmann, R., and Lindquist, S. (2008). Screening for amyloid aggregation by semi-denaturing detergent-agarose gel electrophoresis. J. Vis. Exp. (17), 838.

Halfmann, R., Jarosz, D.F., Jones, S.K., Chang, A., Lancaster, A.K., and Lindquist, S. (2012). Prions are a common mechanism for phenotypic inheritance in wild yeasts. Nature *482*, 363–368.

Hou, F., Sun, L., Zheng, H., Skaug, B., Jiang, Q.X., and Chen, Z.J. (2011). MAVS forms functional prion-like aggregates to activate and propagate antiviral innate immune response. Cell *146*, 448–461.

Hu, Y., Rolfs, A., Bhullar, B., Murthy, T.V., Zhu, C., Berger, M.F., Camargo, A.A., Kelley, F., McCarron, S., Jepson, D., et al. (2007). Approaching a complete repository of sequence-verified protein-encoding clones for Saccharomyces cerevisiae. Genome Res. *17*, 536–543.

Jarosz, D.F., Taipale, M., and Lindquist, S. (2010). Protein homeostasis and the phenotypic manifestation of genetic diversity: principles and mechanisms. Annu. Rev. Genet. *44*, 189–216.

Jarosz, D.F., Brown, J.C., Walker, G.A., Datta, M.S., Ung, W.L., Lancaster, A.K., Rotem, A., Chang, A., Newby, G.A., Weitz, D.A., et al. (2014a). Cross-kingdom chemical communication drives a heritable, mutually beneficial prion-based transformation of metabolism. Cell *158*, 1083–1093.

Jarosz, D.F., Lancaster, A.K., Brown, J.C., and Lindquist, S. (2014b). An evolutionarily conserved prion-like element converts wild fungi from metabolic specialists to generalists. Cell *158*, 1072–1082.

Jones, D.T., and Cozzetto, D. (2015). DISOPRED3: precise disordered region predictions with annotated protein-binding activity. Bioinformatics *31*, 857–863.

Khan, M.R., Li, L., Pérez-Sánchez, C., Saraf, A., Florens, L., Slaughter, B.D., Unruh, J.R., and Si, K. (2015). Amyloidogenic oligomerization transforms Drosophila Orb2 from a translation repressor to an activator. Cell *163*, 1468–1483.

King, C.Y., Tittmann, P., Gross, H., Gebert, R., Aebi, M., and Wüthrich, K. (1997). Prion-inducing domain 2-114 of yeast Sup35 protein transforms in vitro into amyloid-like filaments. Proc. Natl. Acad. Sci. USA *94*, 6618–6622.

Kulak, N.A., Pichler, G., Paron, I., Nagaraj, N., and Mann, M. (2014). Minimal, encapsulated proteomic-sample processing applied to copy-number estimation in eukaryotic cells. Nat. Methods *11*, 319–324.

Kumar, N., Gaur, D., Gupta, A., Puri, A., and Sharma, D. (2015). Hsp90-associated immunophilin homolog Cpr7 is required for the mitotic stability of [URE3] prion in Saccharomyces cerevisiae. PLoS Genet. *11*, e1005567.

Lancaster, A.K., Nutter-Upham, A., Lindquist, S., and King, O.D. (2014). PLAAC: a web and command-line application to identify proteins with prion-like amino acid composition. Bioinformatics *30*, 2501–2502.

Lang, G.I., and Murray, A.W. (2008). Estimating the per-base-pair mutation rate in the yeast Saccharomyces cerevisiae. Genetics *178*, 67–82.

Langkjaer, R.B., Cliften, P.F., Johnston, M., and Piskur, J. (2003). Yeast genome duplication was followed by asynchronous differentiation of duplicated genes. Nature *421*, 848–852.

Langmead, B., and Salzberg, S.L. (2012). Fast gapped-read alignment with Bowtie 2. Nat. Methods *9*, 357–359.

Love, M.I., Huber, W., and Anders, S. (2014). Moderated estimation of fold change and dispersion for RNA-seq data with DESeq2. Genome Biol. *15*, 550.

McGlinchey, R.P., Kryndushkin, D., and Wickner, R.B. (2011). Suicidal [PSI+] is a lethal yeast prion. Proc. Natl. Acad. Sci. USA *108*, 5337–5341.

Nagaraj, N., Kulak, N.A., Cox, J., Neuhauser, N., Mayr, K., Hoerning, O., Vorm, O., and Mann, M. (2012). System-wide perturbation analysis with nearly complete coverage of the yeast proteome by single-shot ultra HPLC runs on a bench top Orbitrap. Mol. Cell Proteomics *11*, M111.013722.

Nakayashiki, T., Kurtzman, C.P., Edskes, H.K., and Wickner, R.B. (2005). Yeast prions [URE3] and [PSI+] are diseases. Proc. Natl. Acad. Sci. USA *102*, 10575–10580.

Ozbudak, E.M., Thattai, M., Lim, H.N., Shraiman, B.I., and Van Oudenaarden, A. (2004). Multistability in the lactose utilization network of Escherichia coli. Nature *427*, 737–740.

Patino, M.M., Liu, J.J., Glover, J.R., and Lindquist, S. (1996). Support for the prion hypothesis for inheritance of a phenotypic trait in yeast. Science *273*, 622–626.

Peelaerts, W., Bousset, L., Van der Perren, A., Moskalyuk, A., Pulizzi, R., Giugliano, M., Van den Haute, C., Melki, R., and Baekelandt, V. (2015). α-Synuclein strains cause distinct synucleinopathies after local and systemic administration. Nature *522*, 340–344.

Prusiner, S.B. (1982). Novel proteinaceous infectious particles cause scrapie. Science *216*, 136–144.

Rechavi, O., Minevich, G., and Hobert, O. (2011). Transgenerational inheritance of an acquired small RNA-based antiviral response in C. elegans. Cell *147*, 1248–1256.

Roberts, B.T., and Wickner, R.B. (2003). Heritable activity: a prion that propagates by covalent autoactivation. Genes Dev. *17*, 2083–2087.

Schulte, T.W., Akinaga, S., Soga, S., Sullivan, W., Stensgard, B., Toft, D., and Neckers, L.M. (1998). Antibiotic radicicol binds to the N-terminal domain of Hsp90 and shares important biologic activities with geldanamycin. Cell Stress Chaperones *3*, 100–108.

Seuring, C., Greenwald, J., Wasmer, C., Wepf, R., Saupe, S.J., Meier, B.H., and Riek, R. (2012). The mechanism of toxicity in HET-S/HET-s prion incompatibility. PLoS Biol. *10*, e1001451.

Shorter, J., and Lindquist, S. (2004). Hsp104 catalyzes formation and elimination of self-replicating Sup35 prion conformers. Science *304*, 1793–1797.

Shorter, J., and Lindquist, S. (2005). Prions as adaptive conduits of memory and inheritance. Nat. Rev. Genet. *6*, 435–450.

Sondheimer, N., and Lindquist, S. (2000). Rnq1: an epigenetic modifier of protein function in yeast. Mol. Cell *5*, 163–172.

Sondheimer, N., Lopez, N., Craig, E.A., and Lindquist, S. (2001). The role of Sis1 in the maintenance of the [RNQ+] prion. EMBO J. *20*, 2435–2442.

Sopko, R., Huang, D., Preston, N., Chua, G., Papp, B., Kafadar, K., Snyder, M., Oliver, S.G., Cyert, M., Hughes, T.R., et al. (2006). Mapping pathways and phenotypes by systematic gene overexpression. Mol. Cell *21*, 319–330.

Suzuki, G., Shimazu, N., and Tanaka, M. (2012). A yeast prion, Mod5, promotes acquired drug resistance and cell survival under environmental stress. Science *336*, 355–359.

Tanaka, M., Chien, P., Naber, N., Cooke, R., and Weissman, J.S. (2004). Conformational variations in an infectious protein determine prion strain differences. Nature *428*, 323–328.

Tapia, H., and Koshland, D.E. (2014). Trehalose is a versatile and long-lived chaperone for desiccation tolerance. Curr. Biol. *24*, 2758–2766.

Ter-Avanesyan, M.D., Dagkesamanskaya, A.R., Kushnirov, V.V., and Smirnov, V.N. (1994). The SUP35 omnipotent suppressor gene is involved in the maintenance of the non-Mendelian determinant [psi+] in the yeast Saccharomyces cerevisiae. Genetics *137*, 671–676.

True, H.L., and Lindquist, S.L. (2000). A yeast prion provides a mechanism for genetic variation and phenotypic diversity. Nature *407*, 477–483.

Uversky, V.N., Oldfield, C.J., Midic, U., Xie, H., Xue, B., Vucetic, S., Iakoucheva, L.M., Obradovic, Z., and Dunker, A.K. (2009). Unfoldomics of human diseases: linking protein intrinsic disorder with diseases. BMC Genomics *10* (*Suppl 1*), S7.

Vavouri, T., Semple, J.I., Garcia-Verdugo, R., and Lehner, B. (2009). Intrinsic protein disorder and interaction promiscuity are widely associated with dosage sensitivity. Cell *138*, 198–208.

Wang, F., Wang, X., Yuan, C.G., and Ma, J. (2010). Generating a prion with bacterially expressed recombinant prion protein. Science *327*, 1132–1135.

Wapinski, I., Pfeffer, A., Friedman, N., and Regev, A. (2007). Natural history and evolutionary principles of gene duplication in fungi. Nature *449*, 54–61.

Ward, J.J., Sodhi, J.S., McGuffin, L.J., Buxton, B.F., and Jones, D.T. (2004). Prediction and functional analysis of native disorder in proteins from the three kingdoms of life. J. Mol. Biol. *337*, 635–645.

Wickner, R.B. (1994). [URE3] as an altered URE2 protein: evidence for a prion analog in Saccharomyces cerevisiae. Science *264*, 566–569.

Wickner, R.B., Edskes, H.K., and Shewmaker, F. (2006). How to find a prion: [URE3], [PSI+] and [beta]. Methods *39*, 3–8.

Winston, F., Dollard, C., and Ricupero-Hovasse, S.L. (1995). Construction of a set of convenient Saccharomyces cerevisiae strains that are isogenic to S288C. Yeast *11*, 53–55.

Wu, H., and Fuxreiter, M. (2016). The structure and dynamics of higher-order assemblies: amyloids, signalosomes, and granules. Cell *165*, 1055–1066.

STAR★METHODS

KEY RESOURCES TABLE

REAGENT or RESOURCE	SOURCE	IDENTIFIER
Antibodies		
Anti-GFP	Roche	Cat#11814460001; RRID: AB_390913
Chemicals, Peptides, and Recombinant Proteins		
Guanidine Hydrochloride	Sigma	Cat#G3272-25G
Hydroxyurea	Sigma	Cat#H8627-1G
Fluconazole	Sigma	Cat#F8929-100MG
Radicicol	Sigma	Cat#R2146-5MG
Paraquat	Sigma	Cat#36541-100MG
Diamide	Sigma	Cat#D3648-1G
Cadmium Chloride	Sigma	Cat#202908-10G
Cobalt Chloride	Sigma	Cat#202185-25G
Copper Sulfate	Sigma	Cat#451657-10G
Manganese Chloride	Sigma	Cat# M8054-100G
Zinc Sulfate	Sigma	Cat# 221376-100G
5-Fluoroorotic Acid	Sigma	Cat# F5013-50MG
Critical Commercial Assays		
RNEasy	QIAGEN	Cat#74104
QuantiTect SYBR Green PCR Kits	QIAGEN	Cat#204141
Deposited Data		
Fungal Orthogroups Repository	Wapinski et al., 2007	http://www.broadinstitute.org/regev/orthogroups
Saccharomyces Genome Database	N/A	http://yeastgenome.org
Experimental Models: Organisms/Strains		
BY4741 mat a	Winston et al., 1995; Brachmann et al., 1998	N/A
BY4742 mat alpha	Winston et al., 1995; Brachmann et al., 1998	N/A
BY4742 *kar1-15*	Conde and Fink, 1976	N/A
Y12	Kruglyak lab	N/A
YJM421	Kruglyak lab	N/A
YJM436	Kruglyak lab	N/A
WE372	Kruglyak lab	N/A
Belgian Ale	White labs	N/A
Y-27788	ARS (NRRL)	http://nrrl.ncaur.usda.gov/index.html
Abbey Ale	White labs	N/A
Urquell Pilsner	Wyeast	N/A
Y-7327	ARS (NRRL)	N/A
Y-12659	ARS (NRRL)	N/A
Y-27806	ARS (NRRL)	N/A
Y-492	ARS (NRRL)	N/A
Y-139	ARS (NRRL)	N/A
OP2	Dietzman, Dietrich	N/A
OP7	Dietzman, Dietrich	N/A
Y-12657	ARS (NRRL)	N/A
Y-1537	ARS (NRRL)	N/A
YB-210	ARS (NRRL)	N/A

(*Continued on next page*)

Continued

REAGENT or RESOURCE	SOURCE	IDENTIFIER
OP8	Dietzman, Dietrich	N/A
ATCC 26249	ARS (NRRL)	N/A
Y-584	ARS (NRRL)	N/A
Y-7115	ARS (NRRL)	N/A
SM69	Dietzman, Dietrich	N/A
Y-162	ARS (NRRL)	N/A
Y-2411	ARS (NRRL)	N/A
Y-269	ARS (NRRL)	N/A
YJM326	Kruglyak lab	N/A
UCD 723	Viticulture and Enology Yeast Culture Collection, UC Davis	http://wineserver.ucdavis.edu/industry/enology/culture/
Recombinant DNA		
Hsp70(K69M) plasmid	Jarosz et al., 2014b	N/A
Advanced Gateway Destination Vectors	Alberti et al., 2007	https://www.addgene.org/yeast-gateway/ Addgene kit # 1000000011
Human ORFeome collection V5.1	CCSB Human ORFeome collection	http://horfdb.dfci.harvard.edu/hv5/
FLEXGene library	Hu et al., 2007	N/A
Sequence-Based Reagents		
oligo-dT(20) primer	Invitrogen	Cat#18418-020
Software and Algorithms		
Disopred2 and Disopred3	Jones and Cozzetto, 2015; Ward et al., 2004	http://bioinf.cs.ucl.ac.uk/psipred/?disopred=1
PLAAC	Lancaster et al., 2014	http://plaac.wi.mit.edu
Matlab	MathWorks, Inc.	http://www.mathworks.com/products/matlab/
Leica LAS X Core Image Analysis Software	Leica, Inc.	http://www.leica-microsystems.com/products/microscope-software/
Bowtie 2.0	Langmead and Salzberg, 2012	http://bowtie-bio.sourceforge.net/bowtie2/index.shtml
DEseq2	Love et al., 2014	https://bioconductor.org/packages/release/bioc/html/DESeq2.html

CONTACT FOR REAGENT AND RESOURCE SHARING

Correspondence and requests for materials should be addressed to Daniel F. Jarosz (danjarosz.aa@gmail.com).

EXPERIMENTAL MODEL AND SUBJECT DETAILS

Yeast strains (Table S5) were obtained from stock centers or generously provided by the sources indicated. All strains were stored as glycerol stocks at −80 °C and revived on YPD before testing. Yeast were grown in YPD at 30 °C unless indicated otherwise. The following media supplements were included where relevant: 3 mM GdHCl, 10 μm radicicol, 1 mg/mL 5-FOA. Yeast were transformed with a standard lithium–acetate protocol (Gietz et al., 1992). First, cells were inoculated and grown to saturation in rich media (YPD). The cells were then diluted and regrown to OD 600nm ~0.8, harvested, washed in sterile water, and resuspended in a transformation master mix (240 μl of PEG 3500 50% w/v, 36 μL1 M LiOAc, 50 μl Boiled SS-Carrier DNA (2mg/mL), 34 μl plasmid DNA (0.1-1 μg), and sterile water to a final volume of 360 μL). Cells were incubated in the transformation master mix at 42°C for 40 min. Following incubation, cells were pelleted, resuspended in 1 ml sterile water, and 10-100 μl was plated on selective medium.

METHOD DETAILS

Yeast Techniques

To eliminate prions chemically, strains were passaged four times on rich medium containing 3 mM GdHCl. To eliminate prions by transient expression of dominant negative Hsp70, cells were transformed with plasmids expressing Hsp70(K69M) from a strong constitutive promoter (GPD) (Jarosz et al., 2014b). Transformants were passaged three times on selective media, followed by

passaging on 5-FOA (for laboratory strains transformed with a URA+ plasmid) or non-selective media (for wild strains transformed with a HPH+ plasmid) to allow for plasmid loss, which was confirmed by the absence of growth on selective media (SD-URA or YPD with hygromycin). Finally, as GdHCl is known to increase the frequencies of petites, all GdHCl-treated isolates were checked for respiration competence on YP-glycerol. To rule out the possibility that the phenotypic states arose from mitochondrial mutations we generated respiration-deficient 'petite' derivatives of representative strains with growth on ethidium bromide. The phenotypic states harbored by these 'petite' strains had the same non-Mendelian inheritance patterns as those harbored by their respiration-competent parents, establishing that the traits did not arise from mitochondrial mutations (Table S4).

For cytoduction experiments, we created a BY4742 strain with a defective KAR allele (*kar1-15*), as an initial recipient for cytoplasmic transfer. This allele prevents nuclear fusion during mating while permitting cytoplasmic transfer. The strain carries auxotrophic markers distinct from those in the putative [*PRION*$^{+}$] donor strains, and was also converted to petite with growth on ethidium bromide. This allowed cytoplasmic transfer to be scored through the restoration of mitochondrial respiration, while selecting for auxotrophic markers unique to the recipient strain. The recipient and donor strains were mixed together on YPD-agar, followed by selection of heterokaryons on dropout media (selecting for the BY4742 recipient strain maker) containing glycerol as a carbon source. One more round of selection was used while replica-plating onto a dual-selection agar plate to confirm that the colonies were not diploids. One additional round of propagation on a non-selective plate was performed before testing ''reverse cytoductions,'' which were performed in the same way except selecting for BY4741 auxotrophy in recipient naive strain. Genetic crosses were performed by mating parental strains on YPD for 6-12 hr, selecting for diploids using auxotrophic markers, and sporulating for 10 days in 10% potassium acetate with 0.5% zinc acetate before isolation of spores with zymolyase digestion and micromanipulation.

Phenotypic assays

For transient overexpression, yeast cells (BY4741 mat A haploids) were transformed with the FLEXGene library. This overexpression library consisted of 5,532 full-length, untagged, sequence-verified, galactose-inducible yeast ORFs in the centromeric plasmid pBY011 (Hu et al., 2007). We pre-grew four biological replicates of the transformed cells for 48 hr in SRaffinose-URA (2% raffinose). We then inoculated 1 μl of these saturated cultures into 384-well plates filled with 45 μl of SGal-URA per well. In parallel we also inoculated analogously prepared 384-well plates containing a variety of stressors in addition to the SGal-URA (UV-irradiation – 80 J/m^2; diamide – 1 mM; paraquat – 0.75 mM; radicicol – 50 μM; fluconazole – 0.2 mM; hydroxyurea – 150 mM; cadmium chloride – 25 μM; cobalt chloride – 1 mM; copper sulfate – 2 mM; manganese chloride – 20 mM; zinc sulfate – 10 mM). Additional stresses in Figure 2 were NaCl – 0.5M; ethanol – 5%; heat – 39°C, acid stress — pH 4, basic stress – pH 9, cetylpyridinium chloride – 1 mM. We grew cells at 30°C in humidified chambers for 48 hr and measured growth by OD_{600} in a microplate reader. We also performed control experiments where we grew the cells in these same conditions but in glucose containing medium (SD-URA) that did not induce gene expression.

We robotically transferred 1 uL of these cultures to new 384-well plates containing 45 uL of SD-URA per well and grew then to saturation over 48 hr at 30°C in humidified chambers. We then repeated the original screening experiment with the same stressors, but this time only in SD-URA. By comparing the growth of cells whose ancestors had experienced protein overproduction and those whose ancestors had not we identified 80 hits that showed the same statistically significant ($p < 0.01$ by t test) phenotypic states in each of the four replicates for further evaluation. For each of these cases we plated ~100 cells from each of the four biological replicates on 5-FOA plates, selected 8-32 individual colonies, and confirmed that they had lost the plasmid. We then grew them in SD-CSM and tested whether they exhibited a phenotype distinct from cells whose ancestors had not experience protein overexpression by examining their growth in the midst of stressors. Cells that harbored such phenotypic states were further examined for characteristics of prion biology (see main text). Wild strains and their chaperone-cured derivatives were phenotyped similarly, in 384-well plates in quadruplicate, but in YPD. Cytoductions were phenotyped in YPD plus/minus stressors in 96-well format and repeated with six biological replicates to confirm reproducibility. Colony morphology was assessed after growth for 7 days at 25°C on YPD plates made with 0.5% agar.

Gene Expression Measurements

Cells harboring phenotypic states and isogenic naive cells were grown in 10 ml YPD cultures and pelleted. We extracted RNA from these pellets using a well-established hot-phenol protocol (Collart and Oliviero, 2001). First, yeast cells were grown to mid-exponential phase (OD600 = 1.0). Cells were collected by centrifugation and washed in cold water. Pellets were resuspended in 400 μl TES solution (10 mM Tris-HCl pH 7.5, 10 mM EDTA, 0.5% SDS), 400 μl acid phenol was added and the mix was vortexed vigorously 10 s. The sample was incubated 30 to 60 min at 65°C with occasional vortexing and then placed on ice for 5 min. Samples were microcentrifuged for 5 min at 20,000 x *g* at 4°C. The aqueous (top) phase was transferred to a clean 1.5 ml microcentrifuge tube and 400 μl acid phenol was added. The tube was vortexed vigorously and spun again. The previous extraction was repeated with chloroform and the aqueous phase was transferred to a new tube, we then added 40 μl of 3M sodium acetate pH 5.3 and 1 ml of cold 100% ethanol, and RNA was precipitated for 1 hr at 80°C. The RNA was microcentrifuged as before, the pellet was washed with cold 70% ethanol, and resupended in water. Extraction was followed by clean up with an RNEasy kit (QIAGEN). We prepared cDNA using an oligo-dT(20) primer (Invitrogen) and SuperScript® Reverse Transcriptase II (Invitrogen), removed residual RNA by enzymatic digestion, and performed quantitative real-time PCR with SYBR green detection (QIAGEN). *ACT1* and/or *TAF10* were used as controls for relative quantification.

Computational Analyses

We examined the amino acid compositions of the proteins from this screen using reported values on the *Saccharomyces* Genome Database (http://www.yeastgenome.org). We calculated disorder scores and profiles using the Disopred2 and Disopred3 algorithms (Jones and Cozzetto, 2015; Ward et al., 2004). Evaluation for canonical prion domains was performed using our published Hidden Markov Model via a webserver (http://plaac.wi.mit.edu)(Lancaster et al., 2014). Orthologs for our hit proteins were selected from a prior analysis of conservation across the fungal lineage based on sequence identity and synteny alike (http://www.broadinstitute.org/regev/orthogroups/)(Wapinski et al., 2007).

Aggregation Assays

SDD–AGE was performed as follows. Yeast were inoculated into 5 mL YPD cultures and incubated 18–24 h at 30°C with 220 rpm agitation. Cells from 1 ml were collected by centrifugation at 3,000 rcf for 2 min, re-suspended in 200 μL sterile water, and then pelleted again by centrifugation. Approximately 100 μL of acid-washed glass beads were then added to each well followed by 80 μL lysis buffer (100 mM Tris pH 8, 1% Triton X-100, 50 mM β-mercaptoethanol, 3% HALT protease inhibitor cocktail, 30 mM N-ethylmaleimide, and 12.5 U ml^{-1} Benzonase nuclease). Blocks were then sealed with a rubber mat (Nunc 276002) and shaken at max speed twice for 3 min on a QIAGEN TissueLyser II. To each well we then added 40 μl 4 × sample buffer (2 × TAE, 20% glycerol, 8% SDS, 0.01% bromophenol blue). The samples was then transferred to individual eppendorf tubes, vortexed briefly, and allowed to incubate at room temperature for three minutes, followed by centrifugation for 2 min at 3,000 rcf to remove cell debris. Electrophoresis and capillary blotting to Hybond ECL nitrocellulose were performed as previously described (Alberti et al., 2010; Halfmann and Lindquist, 2008). Samples were loaded into an agarose gel containing 0.1% SDS. Gel was run at low voltage (< 3V/cm gel length) until dye front was 1cm from the end of the gel (3-4 hr). Blotting paper and nitrocellulose were cut in the same dimensions as the gel and the transfer stack was assembled from the bottom up as follows: 20 pieces of dry GB004 blotting paper, 4 pieces of dry GB002 blotting paper, 1 piece of wet GB002, nitrocellulose, gel (with all bubbles removed), 3 pre-wetted GB002 pieces on top of the gel, and a wick of GB004 on top. The wick was weighted down and each end was submerged in a source of TBS to prevent drying. The transfer was allowed to continue overnight and the nitrocellulose membrane was subsequently processed by a standard Western blotting protocol. Blots were probed with an anti-GFP antibody (Roche 11814460001). Cellulose acetate filter trap assays were performed according to published protocols (Boyé-Harnasch and Cullin, 2006) using lysates prepared as described above. A cellulose acetate membrane (OE66, Schleicher & Schuell) was equilibrated in buffer A containing 2% SDS for 5 min, followed by the recommended assembly of the 96 dot blotting apparatus (Minifold I Dot-Blot System, Schleicher & Schuell). The aggregation assay was carefully opened and 50 μl of each lysate was mixed with 400 μl of buffer A containing 2% SDS. This solution was incubated for 5 min at room temperature and subsequently filtered through the membrane. The samples on the membrane were rinsed twice with 300 μl of buffer A, containing 2% SDS. After releasing from the blotting apparatus, the membrane was rinsed rapidly in desalted water. Subsequently, fluorescence was detected by using VersaDoc, 520LP UV EPI 4 × gain (BioRad).

Microscopy

Microscopy was performed using a Leica inverted fluorescence microscope with a Hammamatsu Orca 4.0 camera. Cells were imaged after growth to exponential phase (OD_{600} of 0.7) in a medium that minimizes autofluorescence (per liter in water: 6.7 g yeast nitrogen base without ammonium sulfate, 5 g casamino acids, 20 g glucose). Exposure time was 1 ms. All images were illumination corrected using standard MATLAB Image Processing Toolbox functions. The background was calculated using a morphological opening with a disk of radius 75 pixels, such that the structuring element was larger than cells in the foreground. Images were first adjusted to a uniform contrast across all images. Images were then manually adjusted to a uniform contrast between each pair of [*PRION*$^+$] and [*prion*$^-$] strains. To justify the choice of a 75 pixel radius structuring element, the Ash 2155 image was background subtracted with radius 15 and 150 structural elements for comparison (Figure S7)

Seeding assays for human orthologs

cDNA of human homologs from Human ORFeome collection V5.1 were cloned into galactose-inducible, 2 micron plasmids with an enhanced GFP tag (Alberti et al., 2007) and transformed into yeast. Transformants were grown to saturation in a low expression medium that did not induce the formation of foci (per liter in water: 6.7 g yeast nitrogen base without ammonium sulfate, 5 g casamino acids, 20 g raffinose or 20 g raffinose + 0.5g galactose) and cells were then imaged 'pre-induction'. Following this, cells were gently spun down, low expression media was removed, and cells were re-suspended in high-expression media (per liter in water: 6.7 g yeast nitrogen base without ammonium sulfate, 5 g casamino acids, 20 g galactose). After 8 hr of induction, the cells were re-imaged. The induced cells were then diluted 200 fold back into low-expression media and allowed to grow for 48 hr to saturation before being imaged one last time. Exposure times were 500 ms.

Lysate Transformations

Lysate transformations were performed as described previously (Du et al., 2010; Tanaka et al., 2004). Briefly 50 ml cultures of donor strains were grown in YPD for 18 hr, pelleted, and washed in H_2O, followed by washing in 1 M sorbitol. The cells were then suspended in 200 μl of SCE buffer (1 M sorbitol, 10 mM EDTA, 10 mM DTT, 100mM sodium citrate, 1 Roche mini-EDTA-free protease inhibitor tablet per 50 mL, pH 5.8) containing 50 units/mL of zymolase 100T. We then incubated the cells for 30 min at 35°C, sonicated them on

ice for 10 s with a sonic dismembrator at 20% intensity, and removed cell debris by centrifugation at 10,000 g at 4°C X 15 min. We then treated these supernatants with excess RNase I and biotinylated DNase (Thermo AM1906) for 1 hr at 37°C. We then removed the DNase by adding saturating quantities of streptavidin-sepharose beads (provided with the biotinylated DNase), incubating for 5 min, and pelleting the beads with centrifugation.

We used these treated supernatants to transform naive recipient yeast spheroplasts. We generated these by first pelleting mid-exponential naive cells, washing them twice in H_2O, followed by washes in 1 M sorbitol. We then re-suspended the cells in 200U/mL zymolyase 100T in 1 M sorbitol and incubated them at 35°C for 15 min. We collected the cells by centrifugation at 600 x *g* for 5 min, washed them with 1 ml sorbitol and then with 1 ml STC buffer (1 M sorbitol, 10 mM $CaCl_2$, 10 mM Tris pH 7.5). Finally, we re-suspended the washed spheroplasts in STC buffer, using wide-mouthed pipet tips to avoid lysis.

We transformed 50 μl aliquots of spheroplasts with 50 μl of lysate, 20 μl salmon sperm DNA (2mg/mL), and 5 μl of a carrier plasmid (URA3- and GFP-expressing pAG426-GFP). We incubated the spheroplasts and lysates for 30 min at room temperature, collected the cells by centrifugation at 600 g X 5 min, and resuspended them in 150ul of SOS-buffer (1 M sorbitol, 7 mM $CaCl_2$, 0.25% yeast extract, 0.5% bacto-peptone. We recovered the spheroplasts at 30°C for 30 min, and plated the entire culture on SD-URA plates overlaid with ~8 ml warm SD-CSM containing 0.8% agar. We incubated the plates at 30°C for 2-3 days, picked dozens of URA+ colonies, and re-streaked them on SD-URA selective media. We then eliminated the carrier plasmid by propagating the colonies on 5-FOA, and tested whether the phenotypic states were transferred from donor to recipient.

QUANTIFICATION AND STATISTICAL ANALYSIS

Quantification and statistical tests employed for each experiment are indicated in the Results section of this paper. We used both unpaired t tests (for comparing measurements from two sets of samples) and Fisher's exact tests (for comparing overlap between sets of proteins and genes). We included all data in these analyses and considered P-values of less than 0.05 significant.

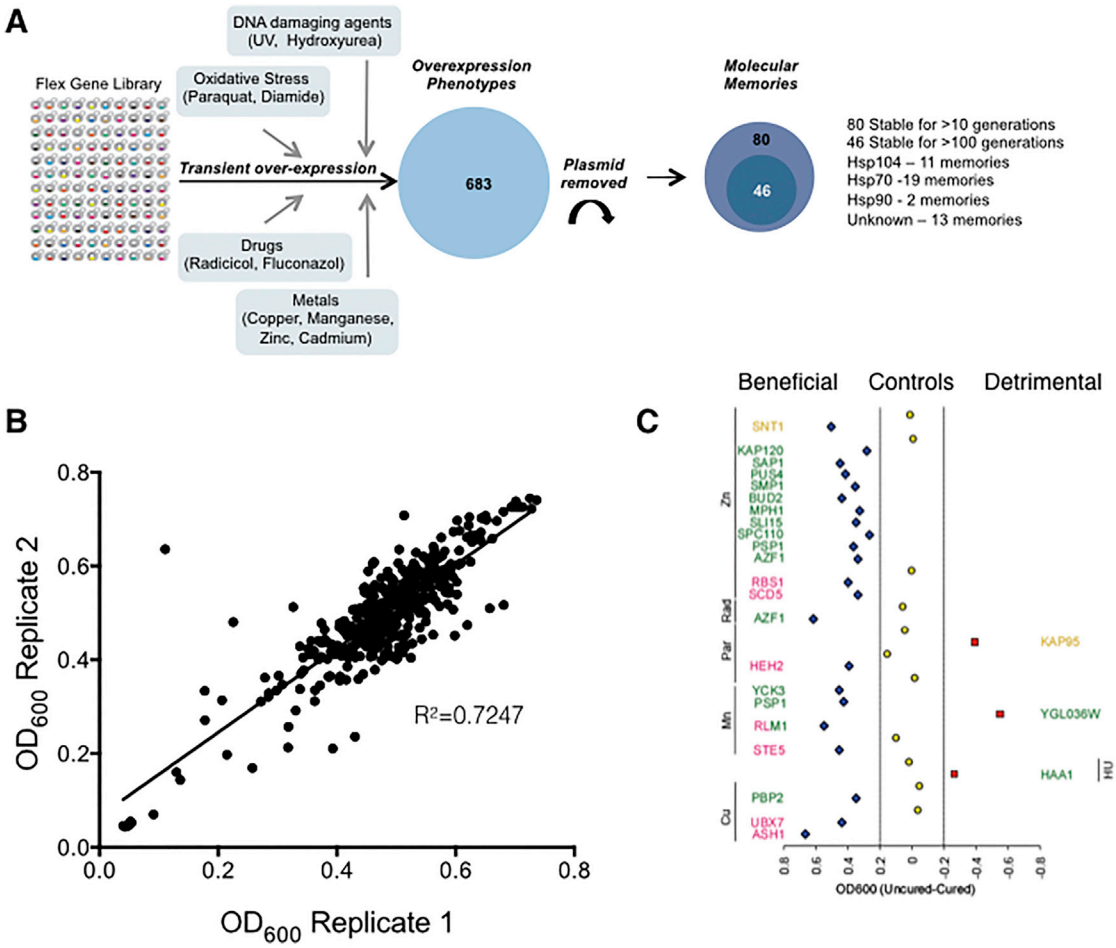

Figure S1. Schematic and Overview of Screen to Identify Heritable Phenotypic States, Related to Figure 1

(A) Schematic of workflow for the screen.

(B) Reproducibility of growth data for a representative plate after re-transformation and re-test. The correlation coefficient between the measurements (R^2 ~0.72) is consistent with what has previously been observed in high throughput overexpression screens.

(C) Overview of the prion-like phenotypic states that emerged from the screen, labeled by their inducing protein and the conditions in which they alter growth. Phenotypic states that were eliminated by transient inhibition of Hsp104 are colored pink, those that were eliminated by transient inhibition of Hsp70 are colored green, and those that were eliminated by transient inhibition of Hsp90 are colored orange. (One of 8 isolates of RLM1 was cured by Hsp104 rather than Hsp70, so it is colored in both green and pink.) A control protein that did not alter phenotypes, DCI1 (yellow), was carried through the screen for each condition and is shown as a control to benchmark the traits produced by the phenotypic states.

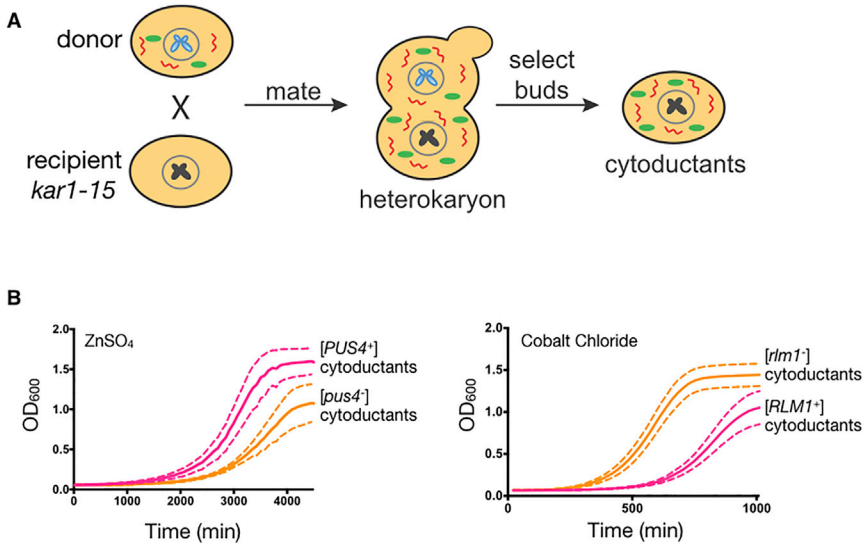

Figure S2. Cytoduction of Phenotypic States, Related to Figure 1

(A) Schematic for cytoduction experiments. Protein-based phenotypic states are depicted by curved red lines, mitochondria by green ovals.

(B) Results from cytoduction of putative [*PUS4*$^{+}$] and [*RLM1*$^{+}$] or naive controls demonstrate that phenotypic states of this type can by transferred cytoplasmically. $ZnSO_4$ tested at 5mM, $CoCl_2$ at 1mM. Dotted lines represent 95% confidence intervals from four biological replicates.

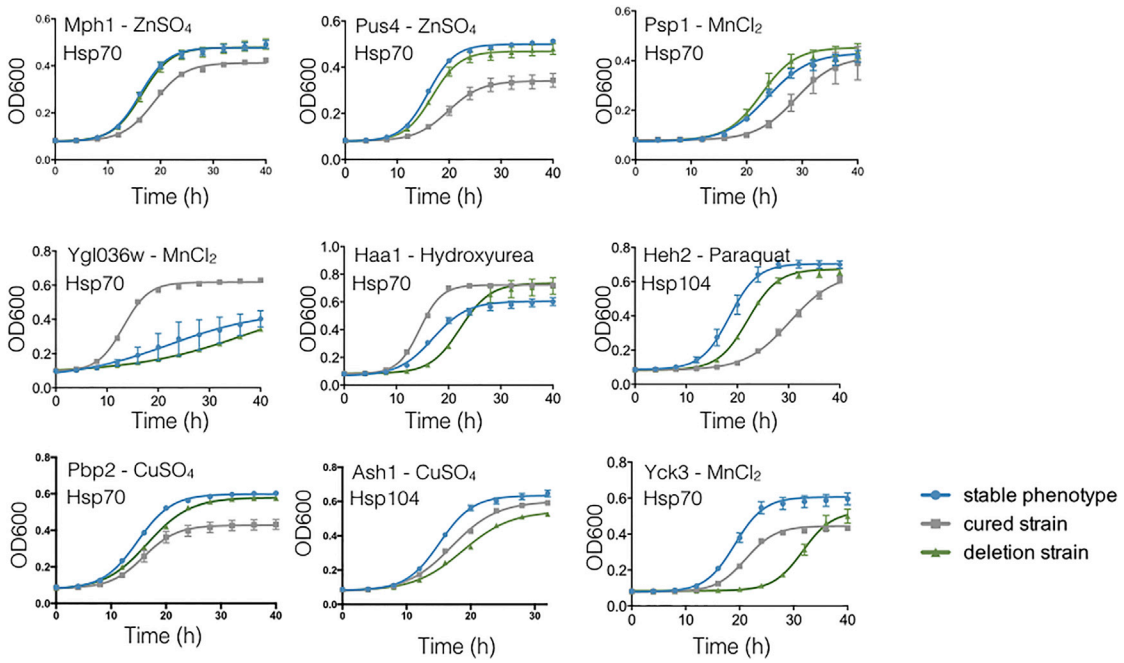

Figure S3. Growth Phenotypes of Additional Phenotypic States Compared to Naive Strains and Strains Harboring Deletions of the Inducing Proteins, Related to Figure 3

Phenotypic states are named by their inducing protein, and growth conditions are indicated on each plot. Error bars are the SEM from three biological replicates.

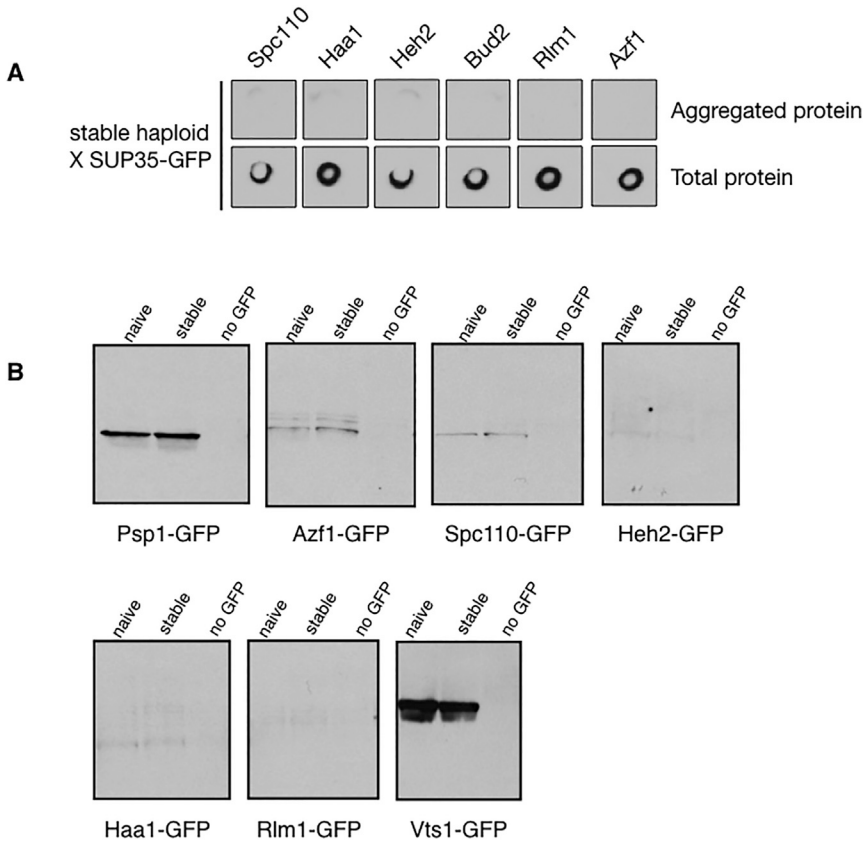

Figure S4. Inducing Proteins Do Not Cross-Seed with Sup35 and Are Expressed at Similar Levels in Naive and Induced Cells, Related to Figure 4

(A) Lysates from diploids harboring the indicated phenotypic states did not seed the assembly of SUP35-GFP into amyloids that could be trapped on cellulose acetate membranes. Diploids were generated by mating haploid cells harboring the indicated phenotypic states to haploid cells expressing Sup35-GFP from its endogenous locus.

(B) Immunoblot of GFP-fusions of inducing proteins in naive cells and cells harboring phenotypic states. Forty micrograms of total protein was loaded per lane. Anti-GFP signal varies according to the endogenous concentrations of each protein. Lane 1 is from a diploid harboring the indicated phenotypic state and a GFP fusion its inducing protein. Lane 2 is from a naive diploid harboring the same GFP fusion. Lane 3 is a control strain with no GFP fusion.

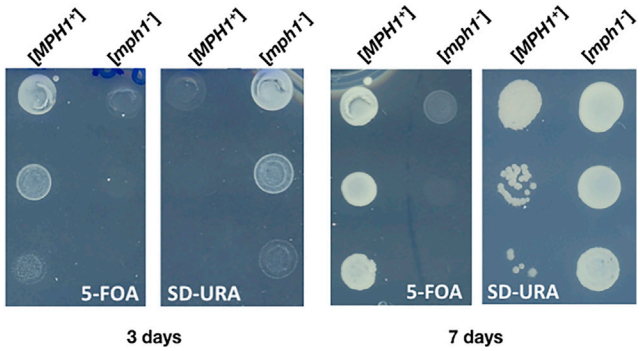

Figure S5. Construction of [*MPH1*$^{+}$] Reporter, Related to Figure 5

A URA3 marker was used to replace the *MDG1* gene, whose expression is downregulated in [*MPH1*$^{+}$] cells. This results in a selectable marker: [*MPH1*$^{+}$] cells grow on media containing 5-FOA but not on SD-URA, whereas [*mph1*$^{-}$] cells grow on media containing 5-FOA but not on SD-URA. Phenotypic repression in [*MPH1*$^{+}$] cells is strong 3 days post-plating, but lessens over time, in contrast to spontaneous mutants, which remain unable to grow on SD-URA.

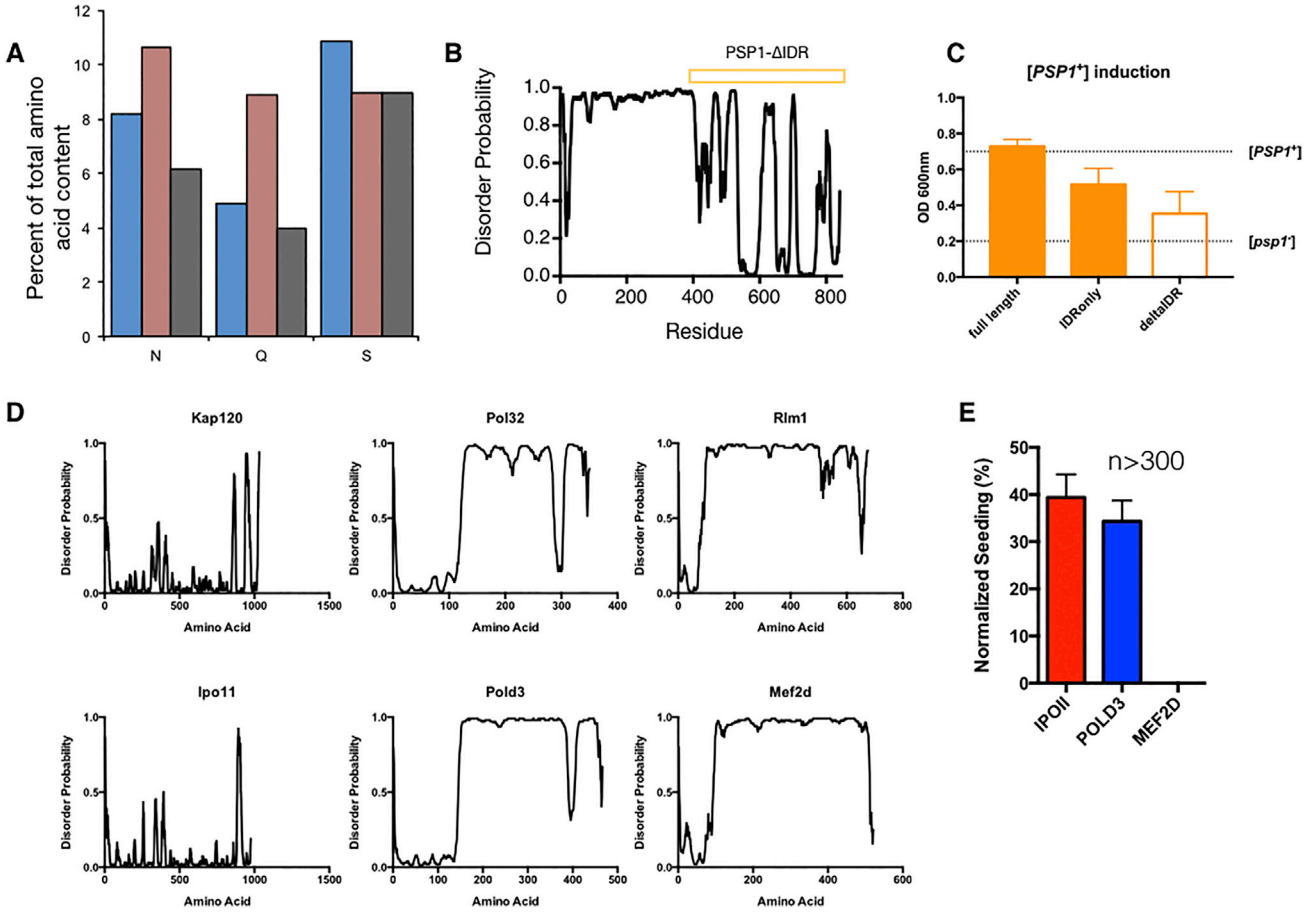

Figure S6. Amino Acid Composition and Disorder Profiles for Inducing Proteins, Related to Figure 7

(A) N, Q, and S composition for the yeast proteome (gray), known prion proteins (salmon), and the hits from this screen (blue).

(B) Disorder profile of Psp1 from *S. cerevisiae* showing the construct delta IDR (containing amino acid residues 450-812) that lacks the intrinsically disordered region.

(C) Delta IDR overexpression did not induce the [*PSP1*$^{+}$] phenotype elicited by a control full-length Psp1 construct tested in parallel. Data from three independently produced [*PSP1*$^{+}$] colonies is also shown for comparison. Error bars represent one SD from three independent biological replicates.

(D) Disorder plots for yeast hits and human homologs tested in the seeding assay.

(E) Quantification of seeding efficiency from the assay.

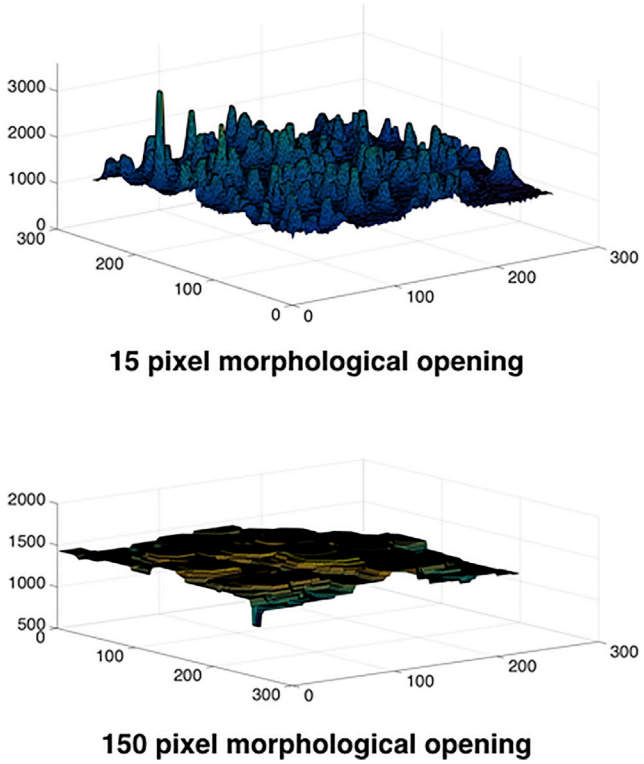

Figure S7. Sample Mask Used for Normalization of Microscope Images, Related to Figure 4 and Microscopy

To justify the choice of a 75 pixel radius structuring element, the Ash 2155 image was background subtracted with radius 15 and 150 structural elements for comparison.